# University of Birmingham

School of Engineering
Department of Mechanical Engineering

**Mechanical Design B (2019-20)**

# Design Group Report

**Design Group No. 47**

Group Members:

| First Name | Surname | ID Number |
|---|---|---|
| Ashan | De Silva | 1768592 |
| Hanxian | Liu | 1742044 |
| Mohammed | Moneeb | 1811551 |
| Vinush | Vigneswaran | 1690302 |

## 1. INTRODUCTION

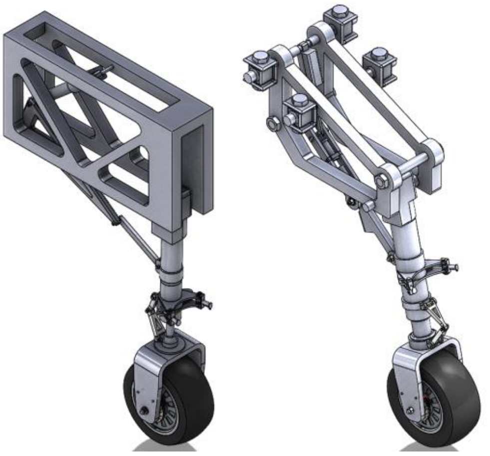

*Figure 1: Initial (left) and final (right) landing gear*

This report will explore the complete analysis and redesign of a retractable nose landing gear to ensure complete feasibility of manufacture and automated assembly. Calculations were carried out for both static and dynamic states, with the aid of Finite Element Analysis of the main loaded components, the quality of the design was evaluated and any points of failure were highlighted. The redesigning of any failing components was carried out to provide a suitable degree of safety. DFA was then carried out by the means of Lucas analysis in which key indices such as handling, fitting and manufacturing cost were used as an assessment criterion for the functionality of the design. From this, the appropriate changes were made, involving a substantial reduction in the number of components, providing an easier assembly process. A second analysis was done as a means of confirming that the redesign was successful. It should be noted that during the redesign process there was a significant increase in the quantity of locating features to allow for complete automated assembly.

## 2. DESIGN FOR SUSTAINABILITY: ANALYSIS

**Table 1: Data required for calculations**

| Part Name | Actuator ($F_{LINK}$) | Up-Lock ($F_{UL}$) | Down-Lock ($F_{DL}$) | Shock Strut ($W_{STRUT}$) | Wheel ($W_{WHEEL}$) | Aircraft ($W_{AIRCRAFT}$) | Torques due to steering |
|---|---|---|---|---|---|---|---|
| **Force/ Moment** | 1260 N | 1400 N | 1400 N | 264 N | 543 N | 14715 N | 15.2 Nm |

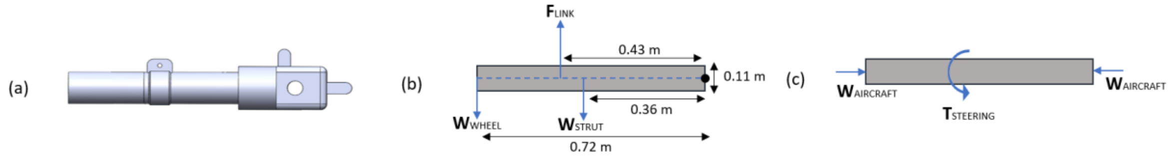


*Figure 2: (a) CAD of strut (b) Free body diagram during actuator retraction. (c) Free body diagram whilst static, and torsion due to steering.*

**2.1. Analysis: Critical Calculations -** Calculations are required to analyse the forces acting on the main strut (shown in figure 2). The main strut is a critical component subjected to the most stress. The following assumptions were made:

- The strut is modelled as a homogenous, simple beam (material: Aluminium 2024, T3).
- The forces are assumed to act on the centre of the beam (the neutral axis).
- Rolling friction at the pivot has been ignored.
- At the instant of initial retraction, it is assumed that the $F_{ACTUATOR}$ is at its maximum.
- The up/down actuator force is considered negligible, as the actuator piston is fully retracted.
- Worst case scenario was taken: full weight of aircraft acts through nose landing gear.

**2.2. Main Strut Stress Analysis (Flexure Formula) -** An analysis of the net moment was calculated, refer to figure 2(b), as follows:

$$(\boldsymbol{Eqn\ 1}) \sum \boldsymbol{M} = (\boldsymbol{W_{STRUT}})(\boldsymbol{D_{P,STRUT}}) - (\boldsymbol{F_{LINK}})\,(\boldsymbol{D_{P,LINK}}) + (\boldsymbol{W_{WHEEL}})(\boldsymbol{D_{P,WHEEL}})$$

$$(Using\ Eqn\ 1) \sum M = (-264)(0.36) + (1260)\,(0.43) + (543)(0.72) = 837.7\ Nm$$

*Where $W_{STRUT}$ = weight of the strut (N), $W_{WHEEL}$, = weight of the wheel and fork (N), $F_{LINK}$ =force caused by the actuator at the link (N), $D_{P,WHEEL}$ = distance from pivot to the wheel (m), $D_{P,LINK}$ = distance from pivot to link and finally (m), $D_{P,STRUT}$ = distance to midpoint of the strut (m).*

$$(\boldsymbol{Eqn\ 2})\ \boldsymbol{I_x} = \frac{\boldsymbol{bh^3}}{\boldsymbol{12}} \qquad (Using\ Eqn\ 2)\ I_x = \frac{(0.72)(0.11)^3}{12} = 7.986\ \times 10^{-5}\ m^4$$

$$(\boldsymbol{Eqn\ 3})\ \boldsymbol{\sigma_x} = \frac{\boldsymbol{My}}{\boldsymbol{I}} \qquad (Using\ Eqn\ 3)\ \sigma_x = \frac{(837.7)(0.055)}{(7.986\ x\ 10^{-5})} = 0.577\ MPa$$

*Where Ix = Second moment of area for rectangle cross-section (m4), b= length of beam (m), h= diameter of beam ($m^4$), $\sigma_x$ = stress (MPa), M = net moment (Nm), y = radius (m).*

**Comment:** The flexure formula shows a high stress at the point of the actuator interface, this can be reduced by increasing the thickness of the beam.

### 2.3. Impact Load & Torsion

$$(\boldsymbol{Eqn\ 4})\ \boldsymbol{F_I} = \sim \boldsymbol{2.5F_{AIRCRAFT}}\ [\boldsymbol{1}] \qquad (Using\ Eqn\ 4)\ F_I = \sim 2.5\ \times 14715 = 36787.5\ N$$

$$(\boldsymbol{Eqn\ 5})\ \boldsymbol{\tau} = \frac{\boldsymbol{Tr}}{\boldsymbol{J}} \qquad (Using\ Eqn\ 5)\ \tau = \frac{(15.2)(0.055)}{(1.44\ \times 10^{-5})} = 0.058\ MPa$$

**Comment:** The impact load is 36787.5 N, therefore the specification for the strut and the shock absorber will be able to withstand the impact load.

### 2.4. Maximum Deflection

$$(\boldsymbol{Eqn\ 6})\ \boldsymbol{\delta_{max}} = \frac{\boldsymbol{P \cdot a^2}}{\boldsymbol{6 \cdot E \cdot I}} \cdot (\boldsymbol{3l - a})\ [\boldsymbol{1}] \qquad \delta = \frac{(453)(0.616)^2(3 \times 0.72 - 0.616)}{(6)(74.6 \times 10^9)(7.986 \times 10^{-5})} = 7.42\ \times 10^{-6}\ m$$

**Comment:** The maximum deflection at the beam is minimal, therefore the strut design required minimal alterations. However, reduction in weight, and change in shape of the shock strut may increase the deflection value.

**2.5. Finite Element Analysis -**Finite element analysis was conducted on the initial design. The material for the strut and the wheel fork is 2024-T3 Aluminium Alloy. This is a common material in aircraft structures, it is desired due to its high fatigue strength and low density. The values of the stress on the FEA simulations, may not be accurate, due to a simple mesh.

**2.5.1. Wheel Bracket Analysis -** The wheel bracket FEA displays high stresses (32.0 MPa) originating at the corners, and decreases along the sides, until it reaches the axle support. It is evident that the lowest stresses are at the fixed point and at the edge axle connection. The factor of safety (10.8) is much larger than required (1.5 - 2.5 meets the requirement for aircraft design [2]), therefore, to reduce the cost of manufacture and mass of component, the wheel bracket material and shape is revised for a lower factor of safety.  A maximum deflection of 0.141 mm was computed.

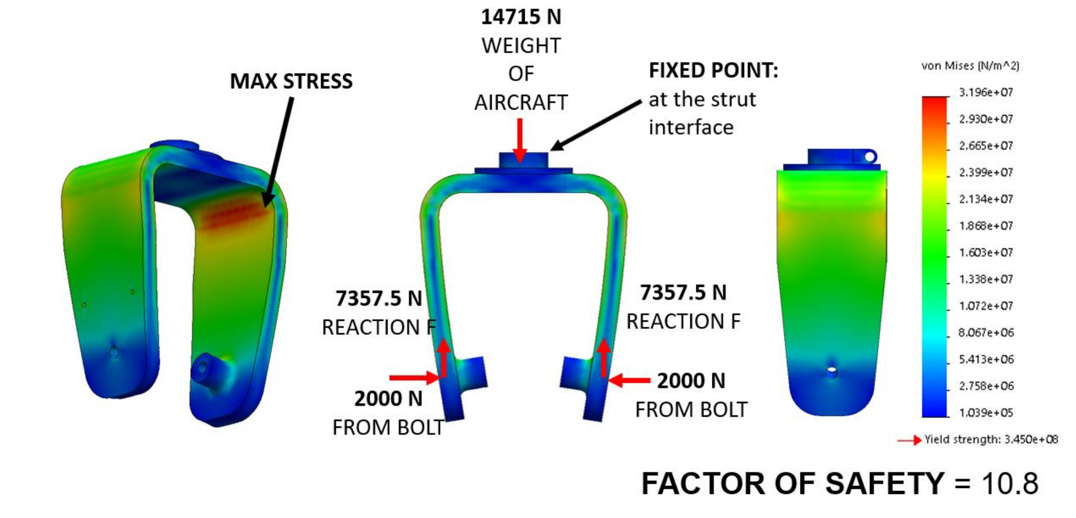


***Figure 3:*** *FEA of wheel bracket with boundary conditions annotated*

**2.5.2. Shock Strut Analysis** - The strut FEA displays highest stress, of 12.2 MPa, at the centre of the beam, when the aircraft is stationary, due to the load from the weight of the aircraft. This stress can be mitigated by increasing the thickness of the hollow shaft. During retraction, in flight, the only force applied is the actuator force, which causes a maximum stress of 5.35 MPa at the interface of the actuator and the shock strut. The factor of safety exceeds the recommended, and will be reduced by changing material, and design change to reduce stress concentrations.

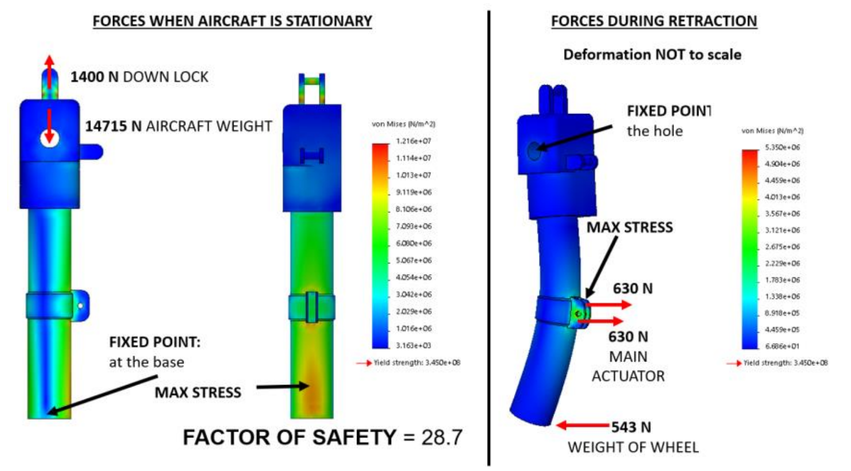


***Figure 4:*** *FEA of shock strut with boundary conditions annotated*

**2.6. Evaluation: Stress Calculations and FEA Simulation**

| | | |
|---|---|---|
| Stress on Strut: | Calculated = 0.577 MPa | FEA = 12.2 MPa |
| Deflection on Strut: | Calculated = 0.00742 mm | FEA = 0.06 mm |

The values of the calculated stress on the strut and FEA simulation show significant discrepancies. The FEA simulation was conducted under a simple mesh, which only considered the forces applied and the geometry of the strut. Similarly, the limitations in the hand calculations, include simplification of the geometry, as a beam. The deflection is greater in the FEA simulation, by a factor of approximately 8, this is because the deflection calculation was made at a point (average of the three-point load). Therefore, the FEA value for the deflection will be closer to the true deflection. The peak stresses in the shock strut is caused by the thin walls, this stress will be mitigated by increasing the thickness, changing the interface with the actuator and the assembly of the landing gear.

## 3. DESIGN FOR SUITABILITY: ANALYSIS

**3.1. Factor of Safety Analysis & Stress Mitigation -** The factor of safety for the strut and the wheel bracket, 28.7 and 10.8 respectively, exceeds the recommended aircraft safety factor of 1.5 to 2.5 [2]. A lower factor safety was achieved by changing the material in correspondence to a lower yield strength. Hence, reducing material and manufacturing cost. Which results in a decrease of the stress propagation on dynamic components. Sharp edges will be chamfered, and complex contours will be avoided. Ribs and gussets may be implemented at the edges and at strut support, to reduce deflection and stress. However, a trade-off between manufacturability, cost and stress mitigation must be considered.

**3.2. Revised Design - Finite Element Analysis -** The material has been changed to 1350 Aluminium Alloy, a cost-effective and lightweight material, which provides a factor of safety used in aerospace industry [3]. The FEA shows that the high stresses have been reduced significantly from the previous design. The revised shock strut design, had a maximum stress of 2.42 MPa, compared to the previous 12.2 MPa (80.1% reduction), and a new factor of safety of 2.1. The revised wheel bracket design has a maximum stress of 18.6 MPa, and the yield strength of the wheel is 27.5 MPa (1350 Aluminium Alloy). The maximum stress has decreased by 41.9%. The wheel bracket has a safety factor of 1.5. The yield strength of the wheel is 27.5 MPa (1350 Aluminium Alloy), however maximum fatigue shown on the wheel bracket is 18.6 MPa, therefore failure is minimised.

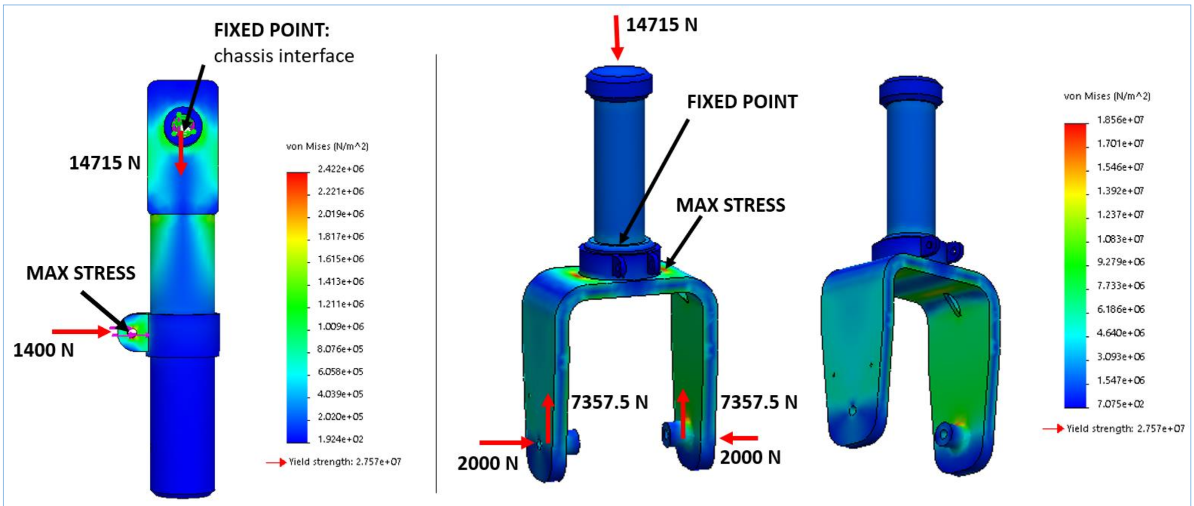

***Figure 5:*** *Revised FEA of shock strut & wheel bracket, with boundary conditions annotated*

## 3.3. Strategy for Redesign

**3.3.1. Wheel Bracket –** The wheel bracket has been merged with the piston of the shock absorber. This reduces the number of components, as well as the stresses applied at the curved surfaces, via dissipating the force over a larger area. Ribs have also been implemented to provide structural support at the locations of failure.

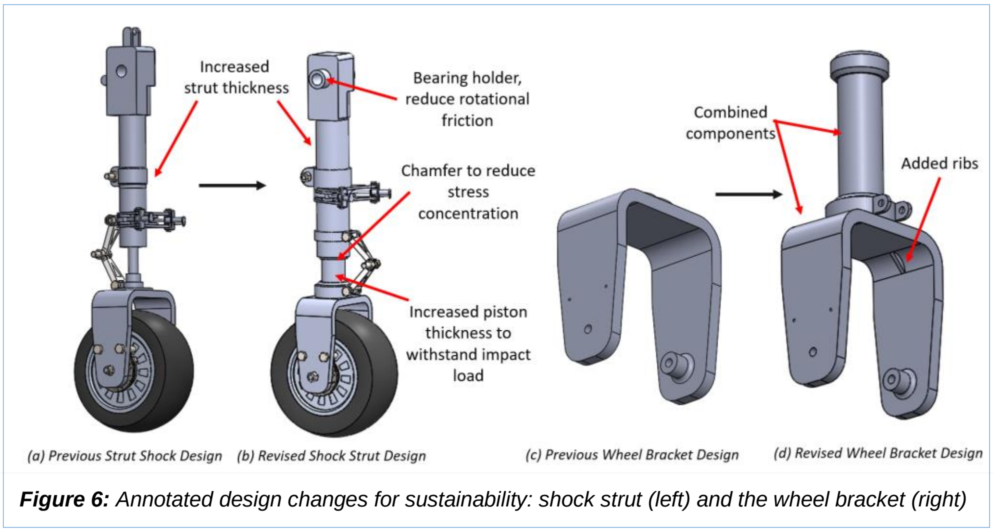

***Figure 6:*** *Annotated design changes for sustainability: shock strut (left) and the wheel bracket (right)*

**3.3.2. Shock Strut –** This structure has been redesigned to reduce stress concentrations by changing from a three-component strut (upper strut, lower strut and shock absorber) to a two-component strut (strut and shock-absorber), figure 6. The FEA analysis showed a large deformation on the strut, due to the actuation force during impact. The thickness of the strut was increased, to withstand the impact load. The strut length had also been increased to hold a larger shock-absorber to account for a safety factor of 1.5. Finally, stress concentrations on the strut had been reduced by introducing chamfers and fillets at sharp edges. Although, this increases the cost of manufacturing, the landing gear is safer for use.

**3.3.3. Chassis -** The mass of the chassis (figure 7) was reduced significantly from, 151.6 kg to 82.3 kg (2024 T3 Aluminium Alloy), without compromising its function, therefore reducing the cost significantly. The new design also allows for a complete retraction of the strut (by an angle of 90$^o$), by increasing the width and reducing the length of the landing gear, therefore making the design more compact. The original design did not consider assembly, it was not possible to interface the actuators and links. Hence, the chassis can now be disassembled easily, and manufactured more efficiently.

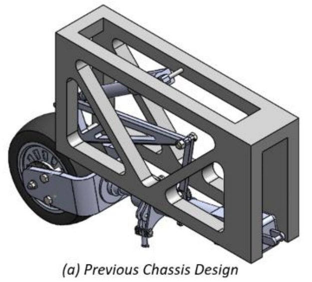

*(a) Previous Chassis Design*

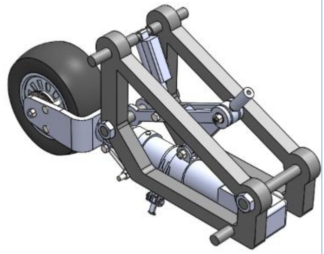

*(b) Revised Chassis Design*

***Figure 7:*** *Chassis redesign*

## 3.4. Conclusion: Design changes for Sustainability & Failure Analysis

The design has been revised for sustainable manufacturing, by reducing the weight of the chassis by 45.7%, in doing so, the required energy over the life-cycle of the chassis decreased, as there are fewer manufacturing processes. The combination of the strut and the wheel bracket reduced the overall stresses at the joint. This increases the power transmission from the steering system, as there are fewer rotating interfaces. A rib structures was implemented at the rounded surface, to prevent failure and minimise deflection. The increase of thickness at the strut has effectively mitigated the stress, as well as provide space for a larger shock absorber. The yield strength of the wheel is 27.5 MPa (1350 Aluminium Alloy), however maximum fatigue shown on the wheel bracket is 18.6 MPa. Similarly, the safety factor for the strut is 2.1, and therefore failure has been minimised.

# 4. SYSTEMS INTERGRATIONS

## 4.1. Bought-out Components Interface & Design Choice

**Table 2: Interfacing strategy and design choice for bough-out components**

| Part No. | Name | Qty | Interface | Design Choice |
|---|---|---|---|---|
| **25** | Tire | 1 | Connected and supported by the wheel | High quality tyre to withstand impact. Tyre width was increased to accommodate increased impact load. |
| **26** | Wheel Rim | 1 | Securely connected to axle & bearing | The wheel is suitable for the selected tyre |
| **29** | Brake Disk | 1 | Securely connected to wheel, via 5 hex bolts. | Hydraulic system to provide reliable and efficient braking. Compact design. |
| **28** | Wheel Bearings 1 | 2 | Connected to axle and wheelbase | Ball bearing as this cheap and reduces the rotational friction efficiently. Easy to assemble. |
| **2** | Ball bearing 2 | 2 | Located at the joint (near up/down actuator). The link arm has been designed to incorporate the bearing. | Reduces rotational friction during operation of main actuator (retraction). Clip-in bearings for ease of assembly. |
| **4** | Main Actuator | 1 | The actuator is attached to the chassis via heavy-duty bolts, and sleeve bearing for | The electromechanical actuator has been chosen due to its robustness, instant response and it is capability of providing |

| | | | | |
|---|---|---|---|---|
| | | | rotation. The actuator is connected the link via bolt and minimal-friction-link. | required power for retraction and deployment. |
| **7** | Up-Down lock actuator | 1 | The up and down lock is located within the link mechanism. The clever design allows for one lock to provide the up-lock and the down lock. | The reduction in complexity of the locks, allows for easy assembly – reduces number of parts required. |
| **16** | Steering Actuators | 2 | The steering mechanism consists of two actuators for the left and right movement – connected to the in-house produces strut and triangle structure. | The steering actuators were chosen based on the required torque. The design is compact. |
| **25** | HEX Bolt BS EN24014 M6 | 5 | Securely attaches braking system, to wheel | The hex bolt selected to connect the supplied disk assembly |
| **26** | HEX Bolt BS EN24014 M6 | 2 | Securely attach the brake callipers to the wheel base. | The hex bolt selected to connect the supplied disk assembly |
| **28** | HEX Bolt BS EN24014 M10 | 3 | Allow for connection of torsion links, with minimum rotational friction. Connected to torsion link joint. | The length of the bolt accommodates the required width of the torsion links and the holder. Provides secure attachment to upper and lower torsion link. Easy assembly procedure. |
| **29** | M50 HEX Bolt | 4 | Allows for secure connection of the support links to the main chassis structure. | Heavy-duty bolts for secure connection. Easy to assemble, requires and Allen key. |
| **30** | M20 HEX Bolt | 1 | Allows for secure connection of up and down lock actuators | Reduces rotational friction during operation and requires Allen key for easy assembly. |
| **31** | HEX Bolt M16 | 1 | Secures actuator linkage, allows for rotation at the strut. | Secure connection, whilst minimising rotational friction. Easy to assemble, requires and Allen key. |
| **32** | HEX Nut (BS EN24014 M10) | 2 | Connected to torsion link joint. | Provides secure attachment to upper and lower torsion link. Easy assembly procedure. |
| **33** | HEX Nut M50 | 4 | Allows for secure connection of the support links to the main chassis structure. | Heavy-duty nuts for secure connection. Easy to assemble, requires and Allen key. |
| **34** | HEX Nut M16 | 1 | Secures actuator linkage, allows for rotation at the strut. | Secure connection, whilst minimising rotational friction. Easy to assemble, requires and Allen key. |

## 4.2. Detailed Sub-Assembly Interfacing (including Airframe Fixture)

<table>
<tr><th>Sub-assemblies:</th><th>Design Evaluation and Interfacing:</th></tr>
<tr><th colspan="2">Chassis</th></tr>
<tr><td>

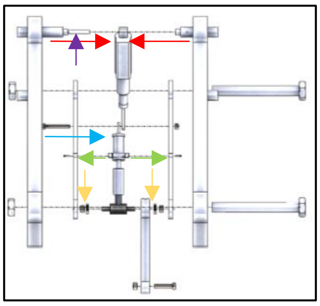

***Figure 8:*** *Chassis and Retraction System*

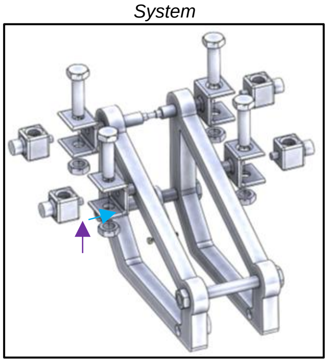

***Figure 9:*** *Chassis and Airframe System*

</td><td>

*<u>Interfacing Chassis and Retraction System:</u>*

**-Main Actuator:** The main actuator situated between the two chassis components, remains axially located using stepped shafts on either side (red arrows in figure 8). This is achieved by having the actuator sit at the point of minimum diameter (Purple arrow), fixing the actuator in place by the increase in radius caused by the steps. Thus, preventing movement along the shaft, securing it onto the outer-chassis without the requirement for any screw fasteners.

**-Locking Actuator**: The up/down-lock actuator (blue arrow) resides within the two upper landing gear levers, making up the inner-chassis, as seen within figure 8. To ensure that the up/down-lock piston can extend into place upon retraction and extension, the actuator must be located to prevent any unwanted longitudinal motion. Hence, it was decided that notches would be put into the upper levers (green arrows) in which the corresponding notches on the cylinder would fit into during assembly, making it self-holding. Therefore, providing location for the two BS EN 24034 M10 Bolts to fix the actuator onto the inner-chassis.

**-Linkages:** During periods of retraction and extension, both the upper and lower levers are required to rotate at different velocities in opposing directions with respect to one another. Single-element ball bearings (yellow arrows) were used to act as an interface between the bearing holder and the upper landing gear levers. This allowed for the bearing holder to rotate with the same angular velocity as the lower lever, and the upper levers to rotate in the opposing direction with an angular velocity equal to that of the outer race of the ball bearing, induced through motion of the main actuator piston.

*<u>Interfacing Chassis and Airframe System:</u>*

**-Airframe**: To secure the landing gear to the airframe, two locking mechanism were placed on either end of the chassis as illustrated in figure 9. To lock the landing gear to the airframe the chassis must be held stationary during assembly. Hence, an interface was used to circumferentially locate the chassis. This consisted of circular perforations (blue arrow) on the outer-chassis with partnering notches on the airframe (purple). These then ensured that all holes were aligned correctly, the landing gear remains fixed, so bolting can be done with ease. It should be noted that the locking joints were placed in accordance with the mass distribution across the landing gear in the retracted position, to reduce any force discrepancies at either joint.

</td></tr>
</table>

<table>
<tr><th>Sub-assemblies:</th><th>Design Evaluation and Interfacing:</th></tr>
<tr><th colspan="2">Strut</th></tr>
<tr><td>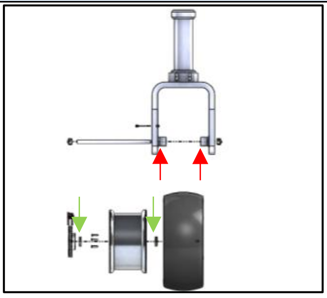<br>***Figure 10:*** *Wheel and Strut System*<br>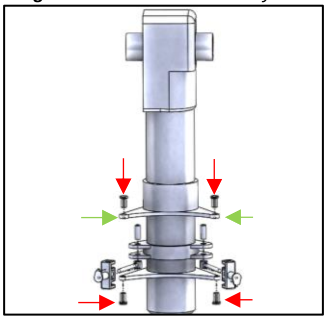<br>***Figure 11:*** *Power Steering and Strut System*</td><td><u>Interfacing between Strut and Wheel:</u><br>-Wheel: Within the design it was imperative that the wheel sub-assembly was located axially to ensure that during complete extension of the landing gear, the wheel does not shift along the axle during motion. This was accomplished by interfacing the two sub-assemblies by ensuring low tolerances between the wheel rim and the bracket during manufacture, using the extrusions illustrated in figure 10 (red arrows).<br>Bracket: Having located the wheel sub-assembly, ball bearings were also used, on either side, as an interface between the wheel axle, rim and bracket (green arrows). This guaranteed that the wheel was able to rotate with minimum restrictions regarding contact surface, and hence reducing rotational fiction.<br><br><u>Interfacing Strut and Power Steering:</u><br>-Power Steering system: To maintain complete functionality of the main shock strut, the power steering sub-assembly had to be both, circumferentially and axially located along the length of the strut. This was achieved without any screws, or bolts, extruding through the cylinder, whereby, the main piston would have to pass for shock absorbance. By merging the upper steering connector on the strut (green arrow, figure 11) during manufacture, the remaining power steering system can be assembled with reference to the merged component. This then allows for complete location using four BS EN 24034 M16 bolts (red arrows), aligning all holes for assembly onto the strut.<br>-Power Steering Actuator: The power Steering actuator is responsible for rotation of the landing gear, which should only move linearly with no circumferential motion within its corresponding cylinder. The pistons were manufactured with shoulders on either side to prevent any rotary motion during extension and retraction, eliminating any torque exerted onto the power steering screws, increasing life span.  Note that this was done for all actuators within the landing gear.</td></tr>
</table>

## 4.3. Summary of Evaluation of Design:

- All actuators will be run electrically, this provides a higher degree of accuracy than other conventional alternatives, ensuring that the landing gear can remain extending or retracted during mechanical failure.
- The final design allows for the assembly of the power steering, wheel and retraction sub-systems prior to fitting to the chassis and strut.
- The final design also allows for fitting to be done using only three unique fasteners with a high tightness of fit, requiring tight and interference fit specifications to keep clearances to a minimum, guaranteeing that all connecting components are fully secured under load.
- The design also includes an extensive number of locating features, allowing for completely automated assembly of all individual sub-systems and complete landing gear.

***NOTE:*** *Exploded View of Final Design (incl. Bill of Materials) – see Appendix D*

***NOTE:*** *Exploded view of Initial Design (incl. Bill of Materials)- see Appendix C*

# 5. EFFECTIVE USE OF DFA (DESIGN FOR ASSEMBLY)

## 5.1. Lucas Analysis: Parameters & Justification for Values - *The complete Lucas Analysis table (with every parameter) can be found in the Appendix A*

**Table 3: Handling, Fitting and Manufacturing Cost Index**

| ITEM NO. | PART NAME | MATERIAL | QTY | ESSENTIAL? | HANDLING INDEX T | FITTING INDEX T | TOLERANCE SURFACE FINISH | BAND | MANUFACTURING COST INDEX Mi |
|---|---|---|---|---|---|---|---|---|---|
| 1 | LANDING GEAR CHASSIS | Aluminum, 2024, T3 | 1 | 0 | 3.3 | 8.2 | >3.0-5.0 | B3 | 161368.38 |
| 2 | LOWER L.GEAR LEVER | Aluminum, A201.0, cast, T7 | 1 | 0 | 1.1 | 7.8 | >0.03-0.05 | B1 | 1281.12 |
| 3 | SHOCK STRUT | Aluminum, 2024, T3 | 1 | 1 | 1.8 | 5.5 | >1.0-3.0 | B4 | 27055.22 |
| 4 | UPPER L.GEAR LEVER | Aluminum, 2024, T3 | 1 | 1 | 1.8 | 9.8 | >0.03-0.05 | B4 | 9000.79 |
| 5 | MAIN ACTUATOR CYLINDER | Aluminum, 6463, T4 | 1 | 1 | 1.3 | 5.6 | >0.01-0.03 | A1 | 5680.00 |
| 6 | MAIN ACTUATOR PISTON | Aluminum, 6463, T4 | 1 | 1 | 1.2 | 5.6 | >0.01-0.03 | A1 | 2021.25 |
| 7 | MAIN ACTUATOR GRIPPER | Aluminum, 6463, T4 | 1 | 1 | 1.1 | 3.3 | >0.15-0.3 | A3 | 1581.34 |
| 8 | UP/DOWN-LOCK HOOK | Aluminum, 2024, T3 | 1 | 1 | 1.5 | 7.7 | >0.15-0.3 | B3 | 2019.98 |
| 9 | UP/DOWN-LOCK CYLINDER | Aluminum, 2024, T3 | 1 | 1 | 2.3 | 10.4 | >0.01-0.03 | A2 | 1944.03 |
| 10 | UP/DPWN-LOCK PISTON | Aluminum, 2024, T3 | 1 | 1 | 2.4 | 7.7 | >0.01-0.03 | A1 | 898.00 |
| 11 | BS EN 24014 - M10 x 45 x 26-B | RS COMPONENTS: 418-8104 | 3 | 0 | 2.3 | 3.2 | - | - | - |
| 12 | BS EN 24034 - M10 - N | RS COMPONENTS: 122-4405 | 4 | 0 | 2.3 | 3.2 | - | - | - |
| 13 | BS EN 24014 - M10 x 70 x 26-B | RS COMPONENTS: 418-8105 | 1 | 0 | 2.3 | 3.2 | - | - | - |
| 14 | BS EN 24014 - M12 x 60 x 30-B | RS COMPONENTS: 508-0994 | 1 | 0 | 2.3 | 1.7 | - | - | - |
| 15 | BS EN 24034 - M12 - N | RS COMPONENTS: 122-4405 | 1 | 0 | 2.3 | 1.7 | - | - | - |
| 16 | SHOCK STRUT PISTON | Aluminum, 2024, T3 | 1 | 1 | 2.2 | 5.5 | >0.01-0.03 | A2 | 2836.99 |
| 17 | SHOCK STRUT CYLINDER | Aluminum, 2024, T3 | 1 | 1 | 1.3 | 9.7 | >0.01-0.03 | A1 | 5843.69 |
| 18 | STEERING CONNECTOR | Aluminum, 2024, T3 | 2 | 1 | 1.3 | 6.8 | >0.8-1.0 | C2 | 1957.24 |
| 19 | STEERING ROTATOR | Aluminum, 2024, T3 | 2 | 1 | 1.3 | 1.8 | >0.8-1.0 | A2 | 2379.84 |
| 20 | UPPER TORQUE LINK | Carbon-fiber-reinforced polymer | 1 | 0 | 1.1 | 7.5 | >3.0-5.0 | B3 | 308.90 |
| 21 | LOWER TORQUE LINK | Carbon-fiber-reinforced polymer | 1 | 0 | 1.1 | 8.1 | >3.0-5.0 | B3 | 314.69 |
| 22 | POWER STEERING CYLINDER | Aluminum, 2024, T3 | 2 | 1 | 1.3 | 7.6 | >0.01-0.03 | A5 | 2719.97 |
| 23 | POWER STEERING PISTON | Aluminum, 2024, T3 | 2 | 1 | 1.3 | 7.0 | >0.01-0.03 | A1 | 880.11 |
| 24 | POWER STEERING SCREW | Cast iron, nodular graphite, EN GJS 800 2 | 2 | 0 | 2.1 | 3.3 | >0.01-0.03 | A1 | 308.44 |
| 25 | BS EN 24014 M10 x 30 x 26-B | RS COMPONENTS: 122 4405 | 4 | 0 | 2.1 | 3.2 | - | - | - |
| 26 | BS EN 24014 - M16 x 100 x 38-N | RS COMPONENTS: 122 4498 | 1 | 0 | 2.1 | 3.2 | - | - | - |
| 27 | BS EN 24034 - M16 - N | RS COMPONENTS: 122 4425 | 1 | 0 | 2.1 | 3.2 | - | - | - |
| 28 | TIRE | Aero trainer (AD4D4) | 1 | 1 | 3.6 | 3.9 | - | - | - |
| 29 | WHEEL RIM | Wheel Wright (TI37-1548) | 1 | 1 | 3 | 3.9 | - | - | - |
| 30 | WHEEL BRACKET | Aluminum, 2024, T3 | 1 | 0 | 1.6 | 2.6 | >1.0-3.0 | B4 | 17746.18 |
| 31 | BRAKE DISC | Tolomatic (0803-1214) | 1 | 1 | 1.5 | 10.4 | - | - | - |
| 32 | BRAKE CALIPER | Tolomatic (H220SAFCIG) | 1 | 1 | 1.8 | 11.1 | - | - | - |
| 33 | PAD NORMAL | Tolomatic (0803-1214) | 2 | 1 | 1.8 | 9.1 | - | - | - |
| 34 | WHEEL AXLE | AISI Type 316L Stainless steel | 1 | 1 | 1.8 | 3.2 | >3.0-5.0 | A1 | 1147.24 |
| 35 | BALL BEARING | RS COMPONENTS: 618-9957 | 2 | 0 | 1.9 | 4.7 | - | - | - |
| 36 | BS EN 24014 - M6 x 30 x 18-B | RS COMPONENTS: 520-144 | 5 | 0 | 2.1 | 1.7 | - | - | - |
| 37 | BS EN 24014 - M6 x 45 x 18-B | RS COMPONENTS: 520-144 | 2 | 0 | 2.1 | 1.7 | - | - | - |
| 38 | BS EN ISO - 4161 - M20 - N | RS COMPONENTS: 508-1307 | 2 | 0 | 2.1 | 1.7 | - | - | - |
| 39 | BS EN 24014 - M16 x 80 x 38-B | RS COMPONENTS: 508-1177 | 1 | 0 | 2.1 | 1.7 | - | - | - |

Table 3 shows a bill of materials for the initial landing gear design. The items highlighted in red are bought-out components, the items highlighted in green are in-house manufactured components. The table illustrates the tolerance/surface finish, as well as the criteria band chosen for each component. The main method of primary material processing was determined by the material, all Aluminium components were forged – this is to reduce the capital cost by having various equipment and machines for primary shaping. The cast iron components were sand casted, as this was cost effective and suitable for the components. Table 3 also shows the essential, (1) and non-essential (0) components, in the 5$^{th}$ column. The essential components were critically chosen based on its importance in delivering the function (retracting, steering and locking). Screws, bolts and nuts were classified as non-essentials.

The values chosen for the feeding and fitting indices were taken from the Lucas Scale table [4]. In order to reduce human errors and subjective values, every member of the group (4+), conducted the handling, fitting and manufacturing cost index – reducing skewed/ biased data. Further information on the choice of feeding and fitting values are given in section 5.2.

## 5.2. Lucas Analysis: Methodology

**5.2.1. Design Efficiency -** The essential and non-essential values were determined by the component requirements for the functionality of the landing gear. The initial Lucas Analysis showed a very low design efficiency: **20.8%.** This was calculated using equation 7.

$$(Eqn\ 7)\ Design\ Efficiency = \frac{\sum Essential\ Components}{\sum Essential\ Components + \sum Non-essential\ Components} \times 100$$

**5.2.2. Manual Feeding/Handling Analysis –** The manual feeding analysis takes into consideration the size and weight of the part [A], the handling difficulties [B], the orientation of the part [C], the rotational orientation of the part [D]. The handling index is simply given by: Handling Index = A+B+C+D, this is conducted for each component. The feeding ratio of the complete assembly is calculated using equation 8.

$$(Eqn\ 8)\ Feeding\ Ratio = \frac{\sum Feeding\ Index}{Essential\ Components} \qquad (Using\ Eqn\ 8)\ Feeding\ Ratio = \frac{115.4}{25} = \mathbf{4.62}$$

**Table 4: Example of Manual Feeding Calculation Results**

| ITEM NO. | PART NAME | MATERIAL | QTY | A | B | C | D | FEEDING INDEX |
|---|---|---|---|---|---|---|---|---|
| 1 | LANDING GEAR CHASSIS | Aluminum, 2024, T3 | 1 | 3 | 0 | 0.1 | 0.2 | 3.3 |

**5.2.3. Manual Fitting Analysis –** The manual fitting analysis considers the part placing and fastening [A], the process direction [B], the insertion type [C], e.g. single, multiple or simultaneous insertion, access/visual to the component [D], alignment [E] and insertion force required [F]. The fitting index is calculated by: Fitting Index = A+B+C+D+E+F. Equation 9, illustrates the calculation for the fitting ratio of the complete assembly.

$$(Eqn\ 9)\ Fitting\ Ratio = \frac{\sum Fitting\ Index}{Number\ of\ Essential\ Components} \qquad (Using\ Eqn\ 9)\ Fitting\ Ratio = \frac{283.3}{25} = \mathbf{11.3}$$

**Table 5: Example of Manual Feeding Calculation Results**

| ITEM NO. | PART NAME | MATERIAL | QTY | A | B | C | D | E | F | FITTING INDEX |
|---|---|---|---|---|---|---|---|---|---|---|
| 1 | LANDING GEAR CHASSIS | Aluminum, 2024, T3 | 1 | 6.0 | 0.0 | 0.7 | 1.5 | 0.0 | 0.0 | 8.2 |

**5.2.4. Manufacturing Cost Index –** The manufacturing cost index is calculated using three indices: relative cost (Rc), the processing cost (Pc) and the material cost (Mc). The relative cost is the product of the complexity factor (Cc), the material factor (Cmp), the minimum section factor (Cs) and the tolerance or finish factor (Ct or Cf). The material cost is calculated as the product of volume of the component (V in mm3), the material cost (Cmt) and the waste coefficient (Wc). Hence, it was calculated using: Mi =(Rc*Pc)+Mc. The manufacturing cost index for the full assembly procedure is the summation of the manufacturing indices for each component.

**Table 6: Example of Manufacturing Cost Index Calculation Results**

| ITEM NO. | PART NAME | MATERIAL | SURFACE / TOLERANCE FINISH | BAND | Cc | Cmp | Cs | Ct or Cf | Pc | V (mm3) | Cmt | Wc | Rc | Mc | MANUFACTURING INDEX |
|---|---|---|---|---|---|---|---|---|---|---|---|---|---|---|---|
| 1 | LANDING GEAR CHASSIS | Aluminum, 2024, T3 | >3.0-5.0 | B3 | 2.2 | 2 | 1 | 1.5 | 151 | 54997181.81 | 0.00243 | 1.2 | 6.6 | 160371.78 | 161368.38 |

**5.3. Lucas Analysis: Key Results –** *The complete Lucas Analysis table can be found in the Appendix A*

**Table 7: Tabulated Key Results**

| Lucas Analysis | Nº Components | Design Efficiency | Feeding Ratio | Fitting Ratio | Sum of Manu Cost Index |
|---|---|---|---|---|---|
| **Initial Design** | 60 | 20.8% | 4.62 | 11.3 | 249293.4 |

**5.4. Evaluation of Lucas Analysis -** The chassis, steering components and actuator mechanism have been completed revised, due to the results of the Lucas Analysis. The Lucas Analysis shows a very inefficient design (20.8%). This is due to the large number of screws, bolts and nuts, which increases the complexity of the assembly procedure, evident by the high feeding and fitting ratios. The revised design takes this into account, and reduces the number of components requiring bolts, screws and nuts. Therefore, reducing the number of non-essential components. The theoretical fitting and feeding ratios should be approximately 1.5 [2][3], however this is unlikely to be achieved in practice. The feeding and fitting ratio of the landing gear were, 4.62 and 11.3 respectively. These were significantly reduced by decreasing the number parts requiring more than one person for manual fitting, designing locating features and symmetrical components. Also, reducing simultaneous multiple insertions, increasing self-holding parts and removing obstructions during assembly (better sub-assembly procedures), all of which can result in optimised fitting and feeding ratios. The manufacturing cost index can be reduced by choosing cheaper manufacturing processes, materials and predominantly weight minimising measures. An example of this was making our chassis smaller, without compromising its function.

# 6. DFA IMPROVEMENTS

## 6.1 Design Choice, DFA analysis, Part Reduction and Functionality Analysis

| **Initial & Redesign Outcome** | **Design Choices Based of DFA and Generated Improvements:** |
|---|---|
| Chassis - **SUCCESS**<br>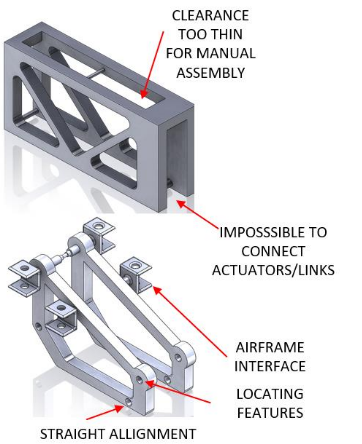<br><br>***Figure 12:*** *Initial (up) and final (down) chassis design* | **a. Design Choice:** The chassis design was altered to reduce the mass significantly. The initial design did not consider the assembly of the actuators and link mechanism interface, as the chassis is closed off. The new simplistic design can be disassembled allowing for the various sub-assembly to be interfaced into the chassis easily. The redesigned chassis, shown in figure 12, also considers interface with the airframe using locking joints.<br><br>**b. DFA Findings:** The manufacturing cost index of the redesigned chassis was significantly lower, 161,000 to 95,000. A reduction of 41.3% was achieved, due to the reduction in the volume of material used (-52%) and the change in the manufacturing process from machining to forging. The handling index reduced, as initially tools were required to reach the chassis components, the new design can be conveniently assembled using hands (robotic or manual). The manual fitting index decreased from 8.2 to 2.2. During assembly, the final design had no restricted access, no visual obstructions, higher number of self-holding components and in-line assembly procedures with single insertion tasks.<br><br>**c. Part Reduction, Functionality Analysis & Life Span:** Although there is an increase in the part number, the functionality of the chassis was improved. The initial design was proved impossible to assemble, with regards to the main actuator mechanism. The life-span of the chassis has been improved, as the new design allows for easier maintenance, and reduced likelihood of damage to component during assembly. |
| Main Actuator Mechanism - **SUCCESS**<br>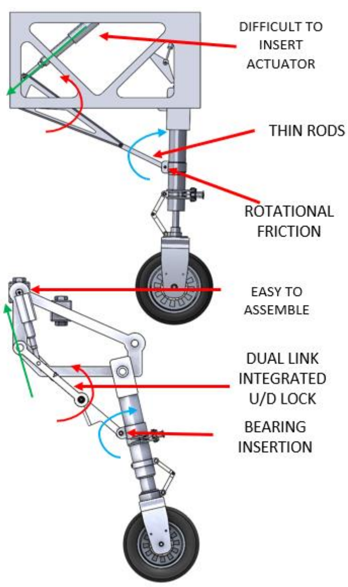<br><br>***Figure 13:*** *Initial (upnd final (down) design* | **a. Design Choice:** The axial positioning of the main retraction actuator was altered on the chassis to reduce the cyclic-loading experienced by both the main and locking actuator, upon retraction and extension. In doing so, the actuator is no longer required to extend for retraction to occur (green arrow). Initially, the strut was unable to fully retract, consuming more volume within the airframe, upon revision, the compact chassis and the actuator positioning allows for a full retraction.<br><br>**b. DFA Findings:** The initial link mechanism to the actuator was difficult to assemble, hence the manual fitting index is high. This was due to the obstruction with the chassis, and the various connection points. The alignment was complex, as each link requires a detachment to interface to the rods within the chassis. This was corrected by having sub-assemblies, and a single connection to the chassis. The new actuator position is easy to access. The feeding index increased, as there are more self-holding components. The link mechanism subassembly simplification was an important contributor in increasing the overall design efficiency.<br><br>**c. Part Reduction & Functionality Analysis:** From the initial to final design of the actuator mechanism, the number of non-essential parts have been reduced, this is because majority of the components in the revised design are self-holding, therefore eliminates the need for additional screws, nuts and bolts. The functionality of the actuator and mechanism has been improved, for lower energy consumption by the main actuator, as well as, achieving a full retraction of the strut. |

<table>
<tr><td>Up/down-Lock Mechanism - SUCCESS<br>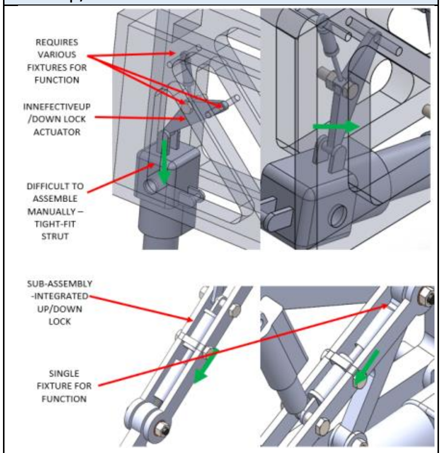<br><br>Figure 14: Initial (up) and final (down) locking mechanism</td>
<td>a. Design Choice: By moving the ineffective up/down lock within the link mechanism, the assembly procedure will be easier and faster as the up/down lock actuator can be assembled separately. Then further assembled with a single connection to the chassis, as opposed to the initial 4 connections. The up/down-lock actuator was not effective in the initial design, as the force applied by the actuator does not lock the strut in place. This has been improved by integrating the actuator with in the link mechanism, as shown in figure 14.<br><br>b. DFA Findings: The manufacturing cost analysis shows a reduction in the cost index after redesign. As the processing cost and waste coefficient have decreased, by 14% and 32% respectively. The simplification of the component from a prismatic part with orthogonal based features to a basic rotational cylindrical feature. This also decreased the manufacturing cost. Fitting index has been reduced due to single insertions (concentric), as opposed to the multiple fixtures to the chassis.<br><br>c. Part Reduction & Functionality Analysis:<br>The reduction of non-essential components due to the initial bolts for the multiple connections was another significant contributor to the increase of the overall design efficiency, from 20.8% to 47.2%. The redesign mechanism improved the functionality of the up/down lock, since it corresponds to a 1.6 factor of safety, whilst securely locking the strut in place.</td></tr>
<tr><td>Strut and Power Steering System - SUCCESS<br>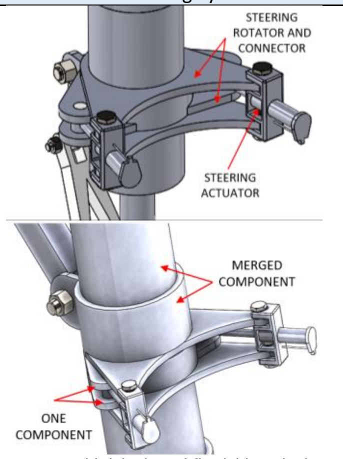<br><br>Figure 15: Initial (up) and final (down) chassis design</td>
<td>a. Design Choice: As shown in figure 15, the two separated steering rotators were merged into a single component. This reduces the complexity of attaching the actuators to the steering rotator. The sleeve was also merged with the main strut, as well as providing a locating feature.<br><br>b. DFA Findings: This significantly reduced the feeding index from 1.8 to 1.3, because the rotational symmetry makes it easier for alignment with the strut. Manual fitting index decreased from 6.8 to 4.1 for the steering connector, as the process has been simplified to a single insertion. Making it easier to align, with a self-holding orientation.<br><br>c. Part Reduction & Functionality Analysis: The parts have been reduced from 6 separate parts to 3 parts, allowing for ease of assembly as well as a reduced number of assembly procedure. The functionality has not been compromised, since the dimension and the interfaces with bought out components have not changed.</td></tr>
<tr><td>Redesign of Steering Mechanism - FAILURE<br>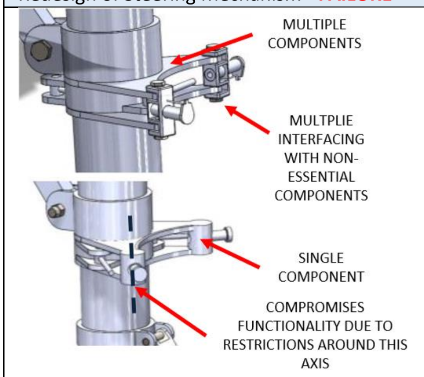<br><br>Figure 16: Initial (up) and final (down) chassis design</td>
<td>An attempt was made, at reducing the number of components by combining the static component of the steering connector and combining the dynamic components of the steering rotator. This potentially would have improved the fitting and feeding indices for the specific parts, however, this would have compromised the functionality of the steering mechanism. This was due to the actuators needing to rotate on its axis during the operation. However, this was inhibited by fixing the actuator position. The new design reduces the lifespan of the actuators, as they would experience high shear stress on its outer shell during extension and retraction. Another issue with the redesigned steering mechanism, was the fixture of the steering connector to the strut, as the combined component makes it impossible to slide the steering component and rotator down the strut. Therefore, it was critical to change the design, as described in figure 15, which was the most feasible solution proposed for reducing the fitting and feeding ratio, whilst improving design efficiency.</td></tr>
</table>

## 6.2. Exploded View of Final Design (including Bill of Materials)

***NOTE:*** *Exploded View of Final Design (incl. Bill of Materials) – see Appendix D*

***NOTE:*** *Exploded view of Initial Design (incl. Bill of Materials)- see Appendix C*

### 6.3. Revised Lucas Analysis (Final Design) - *Complete Lucas Analysis Appendix B*

**Table 8: Handling, Fitting and Manufacturing Cost Index for Final Design**

| ITEM NO. | PART NAME | MATERIAL | QTY | ESSENTIAL? | HANDLING INDEX Total | FITTING INDEX Total | TOLERANCE SURFACE FINISH | BAND | MANUFACTURING COST INDEX Mi |
|---|---|---|---|---|---|---|---|---|---|
| 1 | BS EN 24034 - M20 - N | Stainless steel, austenitic, AISI 302, HT grade B | 4 | 0 | 2.0 | 2.4 | - | - | - |
| 2 | BALL BEARING 2 | RS COMPONENTS: 618-9963 | 2 | 0 | 1.2 | 3.8 | - | - | - |
| 3 | BEARING HOLDER | Cast iron, austempered ductile, ADI 1050 | 1 | 0 | 1.1 | 3.7 | >0.08-0.15 | A1 | 391.83 |
| 4 | MAIN ACTUATOR | Thomson (HD12B160-0400CNO1EEM) | 1 | 1 | 1.3 | 3.3 | - | - | - |
| 5 | UPPER L.GEAR LEVER | Aluminum, 6005, T1 | 2 | 1 | 1.3 | 4 | >1.0-3.0 | B3 | 2660.67 |
| 6 | CHASSIS (RHS) | ALUMINUM 2024-T3 | 1 | 1 | 1.8 | 2.2 | >5.0-10.0 | B4 | 47379.29 |
| 7 | UP/DOWN-LOCK ACTUATOR | Thomson (AA22- 05A65M0M0N) | 1 | 1 | 1.1 | 4 | - | - | - |
| 8 | BS EN 24034 - M16 - N | RS COMPONENTS: 276 768 | 2 | 0 | 2.0 | 3.2 | - | - | - |
| 9 | BS EN 24034 - M10 - B | RS COMPONENTS: 917 3163 | 4 | 0 | 2.0 | 3.2 | - | - | - |
| 10 | LOCKING PISTON HOLDER | Cast iron, austempered ductile, ADI 1050 | 1 | 1 | 1.5 | 2.5 | >0.03-0.05 | A2 | 353.53 |
| 11 | BS EN 24034 - M50 - B | RS COMPONENTS: 917 3019 | 1 | 0 | 1.6 | 2.4 | - | - | - |
| 12 | LOWER L.GEAR LEVER | ALUMINUM 2024-T3 | 1 | 1 | 1.3 | 1.8 | >0.08-0.15 | B4 | 4398.02 |
| 13 | BS EN 24034 - M20 - B | RS COMPONENTS: 508 1307 | 2 | 0 | 2.0 | 1.7 | - | - | - |
| 14 | BS EN 24034 - M16 - B | RS COMPONENTS: 508 1256 | 2 | 0 | 2.0 | 1.7 | - | - | - |
| 15 | SHOCK STRUT | Aluminum ALLOY 1350 | 1 | 1 | 1.3 | 3.3 | >1.0-3.0 | A3 | 35876.06 |
| 16 | STEERING ROTATOR | ALUMINUM 2024-T3 | 1 | 1 | 1.3 | 4.1 | >1.0-3.0 | A2 | 1369.76 |
| 17 | POWER STEERING SCREW | AISI Type 316L Stainless steel | 4 | 0 | 2.0 | 2.5 | >0.08-0.15 | A1 | 83.88 |
| 18 | POWER STEERING ACTUATOR | Thomson (AA42- 21B65M0M0B) | 2 | 1 | 1.3 | 1.8 | - | - | - |
| 19 | STEERING CONNECTOR | AISI Type 316L Stainless steel | 2 | 1 | 1.3 | 2.4 | >1.0-3.0 | C2 | 1457.42 |
| 20 | TORSION LINK CONNECTOR | AISI Type 316L Stainless steel | 2 | 1 | 1.3 | 1.1 | >3.0-5.0 | A2 | 1499.73 |
| 21 | UPPER TORQUE LINK | Carbon-fiber-reinforced polymer | 1 | 1 | 1.1 | 4.8 | >3.0-5.0 | B3 | 308.90 |
| 22 | WHEEL BRACKET | Aluminum ALLOY 1350 | 1 | 0 | 1.8 | 4.1 | >0.03-0.05 | B4 | 28184.17 |
| 23 | LOWER TORQUE LINK | Aluminum ALLOY 1350 | 1 | 1 | 1.1 | 5.4 | >3.0-5.0 | B3 | 314.69 |
| 24 | BS EN 24034 - M10 - N | RS COMPONENTS: 122 4405 | 4 | 0 | 2.0 | 1.7 | - | - | - |
| 25 | TIRE | Aero trainer (AD4D4) | 1 | 1 | 2.1 | 4 | - | - | - |
| 26 | WHEEL RIM | Wheel Wright (TI37-1548) | 1 | 1 | 1.5 | 1.1 | - | - | - |
| 27 | BRAKE CALIPER | Tolomatic (H220SAFCIG) | 1 | 1 | 1.3 | 6.8 | - | - | - |
| 28 | BALL BEARING 1 | RS COMPONENTS: 618-9957 | 2 | 1 | 1.3 | 2.6 | - | - | - |
| 29 | BRAKE DISC | Tolomatic (0803-1214) | 1 | 1 | 1.5 | 1.8 | - | - | - |
| 30 | STRUCT CONNECTOR | Cast iron, austempered ductile, ADI 1050 | 1 | 1 | 1.0 | 3.4 | >3.0-5.0 | A1 | 1147.24 |
| 31 | BS EN 24034 - M50 - N | RS COMPONENTS: 917 3020 | 1 | 0 | 2.0 | 1.7 | - | - | - |
| 32 | CHASSIS (LHS) | Aluminum, 6005, T1 | 1 | 1 | 1.8 | 1.7 | >5.0-10.0 | B4 | 47377.04 |

**Table 9: DFA Key Results Comparison for the Final Design**

| Lucas Analysis | Nº Components | Design Efficiency | Feeding Ratio | Fitting Ratio | Sum of Manufacturing Cost |
|---|---|---|---|---|---|
| **Initial Design** | 60 | 20.8% | 4.62 | 11.3 | 249293.4 |
| **Final Design** | 53 | 47.2% | 3.48 | 5.84 | 172802.2 |
| **Improvement** | +11.7% | 226.9% increase | +24.7% | +48.3% | +30.7% |

### 6.4. Summary of Findings & Evaluation

The design efficiency was increased by 26.4, from 20.8% to 47.2%, by reducing the number of components requiring fastening processes, therefore minimising the need for screws, bolts and nuts. Additionally, the screws were standardised to reduce variety, decreasing the number of fasteners from 12 unique sizes, to 6. The number of components were reduced by 11.7%, by predominantly merging the non-essential components together (e.g. steering rotator and connector), as well as redesigning components to become self-holding, in nature, such as the up/down-lock actuator. Overall, the design was optimised for manual feeding, by dismembering the large non-manufacturable component, e.g. chassis, into smaller feasible sub-components. This allows for manual assembly to be conducted with ease, through reducing handling difficulties. The fitting ratio was refined by simplifying the insertion processes, from simultaneous, multiple insertions to simple, single insertions. Furthermore, the revised design allows for the assembly of the components to be concentric – easy to align.

The DFA was carried out successfully as the initial analysis indicated that the design efficiency was inadequate (20.8%), and therefore a critical evaluation of the bill of materials was conducted. For example, the fitting and feeding ratio of the chassis was, 8.2 and 3.3 respectively, this was a clear indication that a redesign was required of the chassis. The redesign for the chassis was successful, because the fitting and feeding ration decreased to 1.7 and 1.8 respectively. As a by-product of the chassis design change, the manufacturing cost index substantially reduced, from 161,000 to 47,000. This was accomplished by reducing the volume of the material used and minimising the complexity factor. The initial change in the design of the steering mechanism was a failure, as the CAD assembly showed that the main functionality of the steering mechanism will be inhibited, therefore a different approach of merging selected components (e.g the two steering rotators), managed to reduce the fitting, feeding and manufacturing indices. It was concluded, that the complete assembly redesign was effective, because the number of successful design alterations (x12) were much greater than the unsuccessful (x1).

## 7. AUTOMATION OF PRODUCTION

**7.1. Sub-assembly procedure of the Main Actuator Link–** The automated sub-assembly of the main actuator link of the chassis will be discussed in this section. The assembly in figure 17 is suitable for automation due to the simplicity of the process, whereby the sub-tasks includes hole alignment, bolt/screw tightening and concentric insertion of multiple components. This critical sub-assembly has been chosen for automation, as the main chassis and strut assembly will be referenced from this structure. Table 10 shows the functionality and the interface specification of the 8 parts, which was used to design a suitable assembly line, with feasible sensors and robots for efficient assembly. Economical constraints, production rate and suitability of the robots were considered, as shown on table 11.

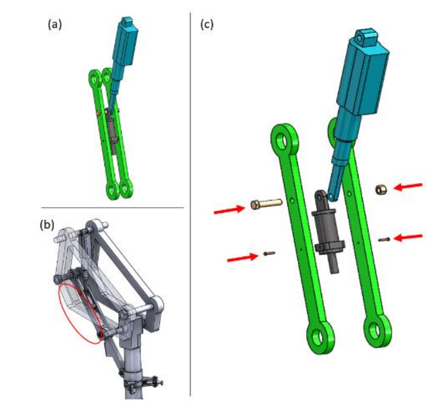


***Figure 17:*** *The sub-assembly of the main actuator, up/down lock actuator and with link mechanism.*

**Table 10: Parts included in the automated sub-assembly**

| Parts No. | Parts Name | A mt | Function & Interface |
|---|---|---|---|
| 4 | Main actuator | x1 | The main electro-mechanical actuator's piston consists of a hole, to interface with the straight bar. |
| 7 | Up/down lock Actuator | x1 | The main up/down actuator's holder consists of a hole, to interface with the straight bar. |
| 5 | Upper L-Gear Lever (Straight bar) | x2 | The holes on in the middle allow for the interface of this sub-assembly. |
| 14 | BS EN 24014 M16 Hex Bolt | x1 | This screw is only threaded at the lower end, low surface roughness in the middle (to reduce rotational friction). Secures the sub-assembly. |
| 9 | BS EN24017 M5 Hex Bolt | x2 | Aligns the up/down lock actuator. |
| 8 | BS EN 24014 M16 Hex Nut | x1 | Fastened to the large screw |

### 7.2. Procedure Block diagram

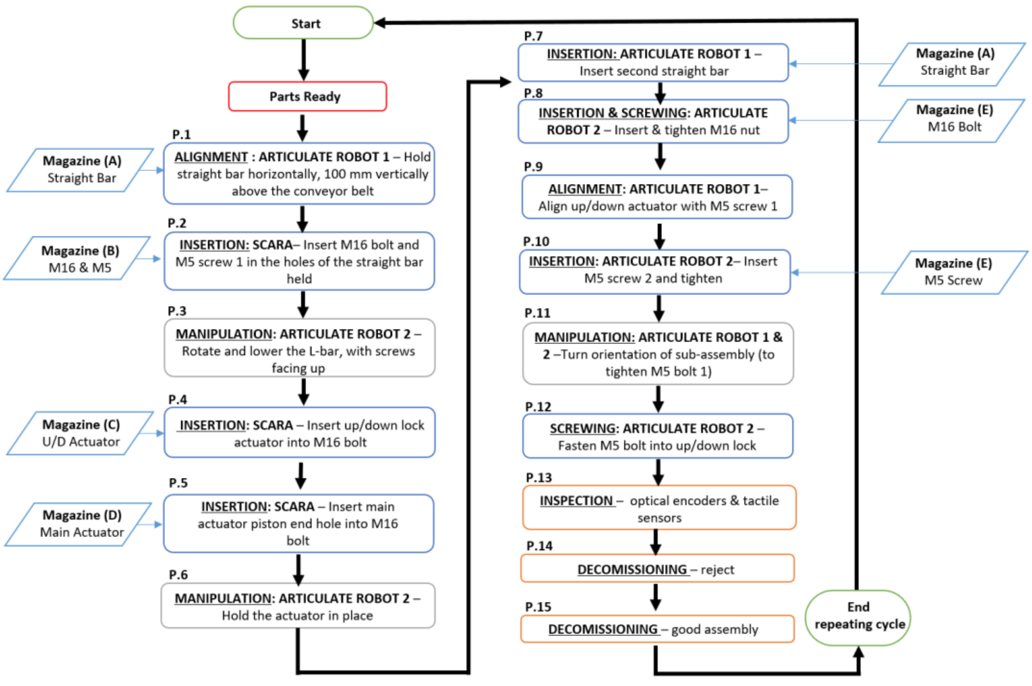


***Figure 18:*** *Step-by-step procedure of assembly of the Main Actuator Link*

### 7.3. Assembly Line: Concept design & Initial Configuration

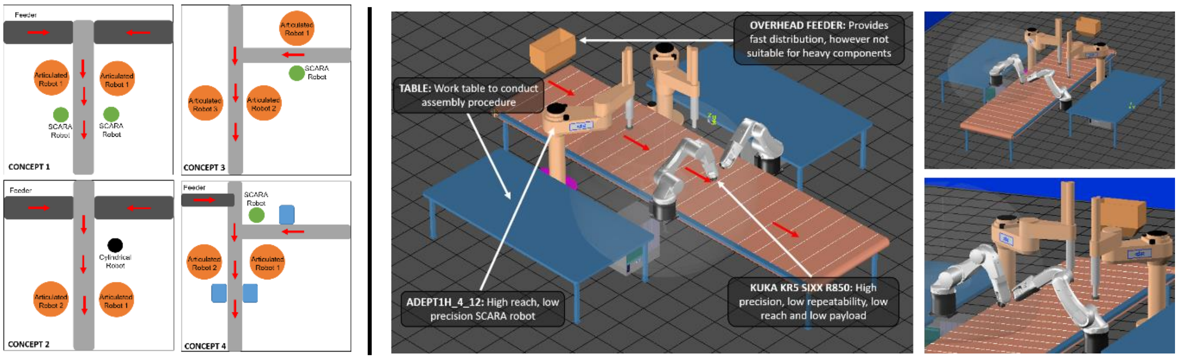


***Figure 19:*** *Four concept designs of assembly line configuration on the left.*

### 7.4. Assembly Line: Optimised Configuration

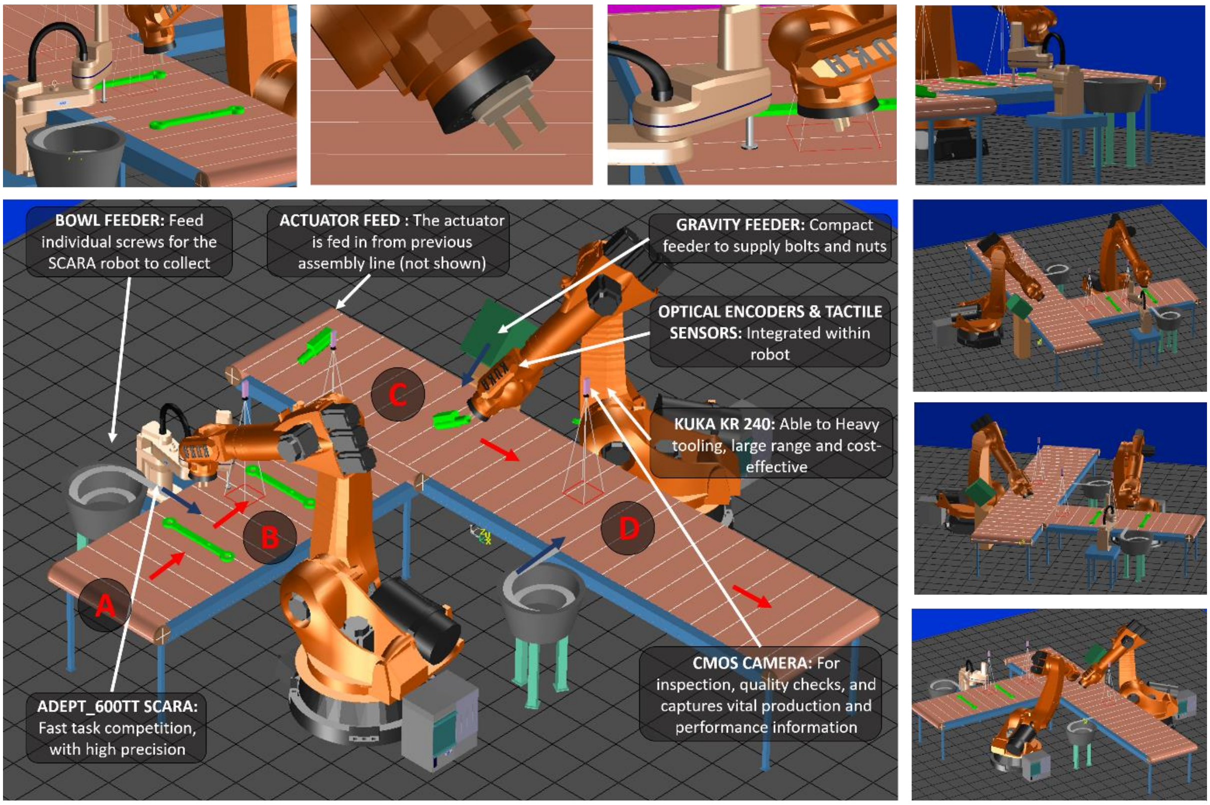


***Figure 20:*** *Optimised assembly line configuration using eHub 27.2. The red arrows show the flow of the main sub-assembly. The blue arrows depict the components being fed from gravity or bowl feeder.*

The flow of of the assembly line is described below (letters refer to figure 20):

**A:** At this location the straight bar enters this section of the subassembly, from a previous manufacturing proves.

**B:** The straight bar stops directly in front of the Articulate Robot 1. The robot lifts the horizontal piece vertically above the conveyor belt, for insertion of bolts by the SCARA robot, which obtains the bolts from the bowl feeder.

**C:** The main actuator is fed through from the second conveyor belt (where the actuator was modified for assembly). The gravity feeder supplies the up/down actuator. Both Articulate Robots work on completing the full assembly, between position C and D.

**D:** The second bowl feeder provides the M16 nuts. The completed part is transported on the conveyor belt to the next workstation for further assembly.

### 7.5. Optimisation of Assembly Procedure

The initial assembly line configuration, in figure 19, was further improved, as shown in figure 20. The following developments were made:

- **Suitability of robot:** The initial robots (KUKA KR5_SIXX) were not suitable for this assembly; the articulate robots' limited reach means more robots are required. KUKA KR 240 provides a larger reach, higher payload, at lower costs.
- **Reduce total work space:** Having a separate table for assembly increases the need for a larger work area, this will increase capital costs. By removing the tables, and conducting the assembly on the conveyor belt, the work space is compact.
- **Minimising time of assembly:** The time of assembly was reduced by grouping the sub tasks, and working collaboratively, in alternating robots between assembly steps.
- **Minimise number of robots:** The change in robot type and configuration allows for the articulate robot 1 to work collaboratively with the SCARA robot and the Articulate Robot 2.
- **Minimise number of steps:** The number of steps has been significantly reduced by grouping task between the three robots, instead of the initial 4 robots. The number of components transferred between the robots has been reduced, decreasing the complexity of the assembly.

### 7.6. Industrial Robot & Suitability after Optimisation

| Assembly Line Specification | | |
|---|---|---|
| **Assembly Description** | The assembly of the main actuator and up/down lock actuator to the straight bar. The block diagram above shows the 15 procedural steps required for the completion of the assembly, inspection and decommissioning. | |
| **Automation Type** | Synchronous transfer systems: the components are transported with an intermittent or discontinuous motion, to allow for the assembly of that certain part. | |
| **Number of Robots** | Total = 3 (2 x KUKA KR 240 and 1 x ADEPT_600TTSCARA) | |
| **Robot Specification** | | |
| **Robot Type** | ADEPT 600TT SCARA | KUKA KR 240 ARTICULATE [5] |
| **Mount** | Table/riser mounted | Floor mounted |
| **Mass** | 41 kg | 1267 kg |
| **End Effector** | Single | Tool Changer: switch between 3 tools: large gripper, smaller gripper and sensor |
| **Payload Analysis** | Maximum pay load =5.5 kg<br>Maximum weight of assembly = 24.3 kg | Maximum pay load =240 kg<br>Maximum weight of assembly = 24.3 kg |
| **Maximum Reach** | 0.6 m | 2.7 m |
| **Work Volume** | 0.24 $m^2$ | 82.45 $m^3$ |
| **Capital Cost** | £11,800 | £9,500 |
| **Evaluation of Suitability** | • **Synchronous transfer system:** This automation eliminates the need for a table workstation, the process of assembly can be conducted on the conveyor belt. Minimising time of completion of sub-tasks, therefore increasing production rate.<br>• **KUKA KR 240**: This is suitable for this assembly due to its large load-bearing capacity (240 kg), therefore able to carry the straight bar (24.3 kg). Any changes to the link mechanism, or chassis, can be easily accommodated by this versatile robot. The work volume of the robot is high, as the articulate robot 1, works in collaboration with both SCARA and Articulate Robot 2, in two different conveyor belts. The high reach of this robot, reduces the number of robots required, therefore the assembly is conducted with low capital cost.<br>• **ADEPT 600TT SCARA:** The fast-sustained cycle time (0.64 s) reduces delays during alignment and bolt fittings. The small work volume, ensures there is no contact between the two robots. This robot also provides precision when inserting bearings/ or bolts, as well as accurate alignment. | |

**Table 11: Assembly line specification and robot specification**

## 8. REFERENCES

[1 ] Shigley, J.E., 2011. Shigley's mechanical engineering design. Tata McGraw-Hill Education.

[2] United States. Army. Air Corps (2005). Structural analysis and design of airplanes. Palm Springs, Ca: Wexford College Press.-Factor of safety value

[3] Parashar, B.N. and Mittal, R.K., 2002. Elements of manufacturing processes. PHI Learning Pvt. Ltd..-Factor of Safety Reference

[4] Swift, K.G. and Booker, J.D., 2003. Process selection: from design to manufacture. Elsevier.-Lucas Reference

[5] K'Nevez, J.Y., Cherif, M., Zapciu, M. and Gérard, A., 2012. Experimental characterization of robot arm rigidity in order to be used in machining operation. arXiv preprint arXiv:1201.4445.

# APPENDIX A – Lucas Analysis Detailed Calculation Table

| ITEM NO. | PART NAME | MATERIAL | DENSITY | MASS | QTY | ESL | HANDLING INDEX | | | | | FITTING INDEX | | | | | | | TOLERANCE | BAND | Rc | | | | Pc | Mc | | | MANUFACTURING COST INDEX | | |
|---|---|---|---|---|---|---|---|---|---|---|---|---|---|---|---|---|---|---|---|---|---|---|---|---|---|---|---|---|---|---|---|
| | | | kg/m3 | kg | | | A | B | C | D | T | A | B | C | D | E | F | T | SURFACE FINISH | | Cc | Cmp | Cs | Ct or Cf | | Volume (mm3) | Cmt | Wc | Rc | Mc | Mi |
| 1 | LANDING GEAR CHASSIS | Aluminum, 2024, T3 | 2750 | 151.24 | 1 | 0 | 3 | 0 | 0.1 | 0.2 | 3.3 | 6.0 | 0.0 | 0.7 | 1.5 | 0.0 | 0.0 | 8.2 | >3.0-5.0 | B3 | 2.2 | 2 | 1 | 1.5 | 151 | 54997181.81 | 0.00243 | 1.2 | 6.6 | 160371.78 | 161368.38 |
| 2 | LOWER L.GEAR LEVER | Aluminum, A201.0, cast, T7 | 2780 | 0.58 | 1 | 0 | 1 | 0 | 0.1 | 0 | 1.1 | 3.3 | 1.6 | 0.7 | 1.5 | 0.7 | 0.0 | 7.8 | >0.03-0.05 | B1 | 1 | 2 | 1 | 2.4 | 151 | 208125.66 | 0.00243 | 1.1 | 4.8 | 556.32 | 1281.12 |
| 3 | SHOCK STRUT | Aluminum, 2024, T3 | 2750 | 24.20 | 1 | 1 | 1.5 | 0 | 0.1 | 0.2 | 1.8 | 1.0 | 1.6 | 0.7 | 1.5 | 0.7 | 0.0 | 5.5 | >1.0-3.0 | B4 | 2.3 | 2 | 1 | 2 | 151 | 8801790.33 | 0.00243 | 1.2 | 9.2 | 25666.02 | 27055.22 |
| 4 | UPPER L.GEAR LEVER | Aluminum, 2024, T3 | 2750 | 6.92 | 1 | 1 | 1.5 | 0 | 0.1 | 0.2 | 1.8 | 6.0 | 1.6 | 0.7 | 1.5 | 0.0 | 0.0 | 9.8 | >0.03-0.05 | B4 | 2.3 | 2 | 1 | 2.4 | 151 | 2515002.36 | 0.00243 | 1.2 | 11.04 | 7333.75 | 9000.79 |
| 5 | MAIN ACTUATOR CYLINDER | Aluminum, 6463, T4 | 2660 | 4.81 | 1 | 1 | 1 | 0 | 0.1 | 0.2 | 1.3 | 3.3 | 0.1 | 0.7 | 1.5 | 0.0 | 0.0 | 5.6 | >0.01-0.03 | A1 | 1 | 2 | 1 | 2.8 | 151 | 1808606.31 | 0.00243 | 1.1 | 5.6 | 4834.40 | 5680.00 |
| 6 | MAIN ACTUATOR PISTON | Aluminum, 6463, T4 | 2660 | 1.17 | 1 | 1 | 1 | 0.2 | 0 | 0 | 1.2 | 3.3 | 0.1 | 0.7 | 1.5 | 0.0 | 0.0 | 5.6 | >0.01-0.03 | A1 | 1 | 2 | 1 | 2.8 | 151 | 439822.97 | 0.00243 | 1.1 | 5.6 | 1175.65 | 2021.25 |
| 7 | MAIN ACTUATOR GRIPPER | Aluminum, 6463, T4 | 2660 | 0.24 | 1 | 1 | 1 | 0 | 0.1 | 0 | 1.1 | 1.0 | 0.1 | 0.7 | 1.5 | 0.0 | 0.0 | 3.3 | >0.15-0.3 | A3 | 2.3 | 2 | 1 | 1.9 | 151 | 89710.92 | 0.00243 | 1.2 | 8.74 | 261.60 | 1581.34 |
| 8 | UP/DOWN-LOCK HOOK | Aluminum, 2024, T3 | 2750 | 0.71 | 1 | 1 | 1 | 0 | 0.1 | 0.4 | 1.5 | 3.3 | 1.6 | 0.7 | 1.5 | 0.0 | 0.6 | 7.7 | >0.15-0.3 | B3 | 2.2 | 2 | 1 | 1.9 | 151 | 259816.27 | 0.00243 | 1.2 | 8.36 | 757.62 | 2019.98 |
| 9 | UP/DOWN-LOCK CYLINDER | Aluminum, 2024, T3 | 2750 | 0.17 | 1 | 1 | 1.5 | 0.4 | 0 | 0.4 | 2.3 | 6.0 | 1.6 | 0.7 | 1.5 | 0.0 | 0.6 | 10.4 | >0.01-0.03 | A2 | 2.1 | 2 | 1 | 2.8 | 151 | 62950.92 | 0.00243 | 1.1 | 11.76 | 168.27 | 1944.03 |
| 10 | UP/DPWN-LOCK PISTON | Aluminum, 2024, T3 | 2750 | 0.05 | 1 | 1 | 1.5 | 0.4 | 0.1 | 0.4 | 2.4 | 3.3 | 1.6 | 0.7 | 1.5 | 0.0 | 0.6 | 7.7 | >0.01-0.03 | A1 | 1 | 2 | 1 | 2.8 | 151 | 19603.36 | 0.00243 | 1.1 | 5.6 | 52.40 | 898.00 |
| 11 | BS EN 24014 - M10 x 45 x 26-B | RS COMPONENTS: 418-8104 | - | - | 3 | 0 | 1.5 | 0.3 | 0.1 | 0.4 | 2.3 | 1.0 | 0.1 | 0.0 | 1.5 | 0.0 | 0.6 | 3.2 | - | - | - | - | - | - | - | - | - | - | - | - | - |
| 12 | BS EN 24034 - M10 - N | RS COMPONENTS: 122-4405 | - | - | 4 | 0 | 1.5 | 0.3 | 0.1 | 0.4 | 2.3 | 1.0 | 0.1 | 0.0 | 1.5 | 0.0 | 0.6 | 3.2 | - | - | - | - | - | - | - | - | - | - | - | - | - |
| 13 | BS EN 24014 - M10 x 70 x 26-B | RS COMPONENTS: 418-8105 | - | - | 1 | 0 | 1.5 | 0.3 | 0.1 | 0.4 | 2.3 | 1.0 | 0.1 | 0.0 | 1.5 | 0.0 | 0.6 | 3.2 | - | - | - | - | - | - | - | - | - | - | - | - | - |
| 14 | BS EN 24014 - M12 x 60 x 30-B | RS COMPONENTS: 508-0994 | - | - | 1 | 0 | 1.5 | 0.3 | 0.1 | 0.4 | 2.3 | 1.0 | 0.1 | 0.0 | 0.0 | 0.0 | 0.6 | 1.7 | - | - | - | - | - | - | - | - | - | - | - | - | - |
| 15 | BS EN 24034 - M12 - N | RS COMPONENTS: 122-4405 | - | - | 1 | 0 | 1.5 | 0.3 | 0.1 | 0.4 | 2.3 | 1.0 | 0.1 | 0.0 | 0.0 | 0.0 | 0.6 | 1.7 | - | - | - | - | - | - | - | - | - | - | - | - | - |
| 16 | SHOCK STRUT PISTON | Aluminum, 2024, T3 | 2750 | 1.09 | 1 | 1 | 1.5 | 0.2 | 0.1 | 0.4 | 2.2 | 3.3 | 1.6 | 0.0 | 0.0 | 0.0 | 0.6 | 5.5 | >0.01-0.03 | A2 | 2.1 | 2 | 1 | 2.8 | 151 | 397018.77 | 0.00243 | 1.1 | 11.76 | 1061.23 | 2836.99 |
| 17 | SHOCK STRUT CYLINDER | Aluminum, 2024, T3 | 2750 | 5.14 | 1 | 1 | 1 | 0 | 0.1 | 0.2 | 1.3 | 6.0 | 1.6 | 0.0 | 1.5 | 0.0 | 0.6 | 9.7 | >0.01-0.03 | A1 | 1 | 2 | 1 | 2.8 | 151 | 1869842.64 | 0.00243 | 1.1 | 5.6 | 4998.09 | 5843.69 |
| 18 | STEERING CONNECTOR | Aluminum, 2024, T3 | 2750 | 0.37 | 2 | 1 | 1 | 0 | 0.1 | 0.2 | 1.3 | 6.0 | 0.1 | 0.0 | 0.0 | 0.7 | 0.0 | 6.8 | >0.8-1.0 | C2 | 2.2 | 2 | 1 | 2.4 | 151 | 135683.49 | 0.00243 | 1.1 | 10.56 | 362.68 | 1957.24 |
| 19 | STEERING ROTATOR | Aluminum, 2024, T3 | 2750 | 0.88 | 2 | 1 | 1 | 0 | 0.1 | 0.2 | 1.3 | 1.0 | 0.1 | 0.0 | 0.0 | 0.7 | 0.0 | 1.8 | >0.8-1.0 | A2 | 2.1 | 2 | 1 | 2.4 | 151 | 320898.32 | 0.00243 | 1.1 | 10.08 | 857.76 | 2379.84 |
| 20 | UPPER TORQUE LINK | Carbon-fiber-reinforced polymer | 1100 | 0.11 | 1 | 0 | 1 | 0 | 0.1 | 0 | 1.1 | 6.0 | 0.1 | 0.7 | 0.0 | 0.7 | 0.0 | 7.5 | >3.0-5.0 | B3 | 1.8 | 1.5 | 1 | 1 | 100 | 101034.04 | 0.00035 | 1.1 | 2.7 | 38.90 | 308.90 |
| 21 | LOWER TORQUE LINK | Carbon-fiber-reinforced polymer | 1100 | 0.13 | 1 | 0 | 1 | 0 | 0.1 | 0 | 1.1 | 6.0 | 0.1 | 0.7 | 0.0 | 0.7 | 0.6 | 8.1 | >3.0-5.0 | B3 | 1.8 | 1.5 | 1 | 1 | 100 | 116079.66 | 0.00035 | 1.1 | 2.7 | 44.69 | 314.69 |
| 22 | POWER STEERING CYLINDER | Aluminum, 2024, T3 | 2750 | 0.16 | 2 | 1 | 1 | 0 | 0.1 | 0.2 | 1.3 | 6.0 | 1.6 | 0.0 | 0.0 | 0.0 | 0.0 | 7.6 | >0.01-0.03 | A5 | 3 | 2 | 1 | 2.8 | 151 | 57983.44 | 0.00243 | 1.3 | 16.8 | 183.17 | 2719.97 |
| 23 | POWER STEERING PISTON | Aluminum, 2024, T3 | 2750 | 0.04 | 2 | 1 | 1 | 0.2 | 0.1 | 0 | 1.3 | 3.3 | 1.6 | 0.0 | 1.5 | 0.0 | 0.6 | 7.0 | >0.01-0.03 | A1 | 1 | 2 | 1 | 2.8 | 151 | 12910.53 | 0.00243 | 1.1 | 5.6 | 34.51 | 880.11 |
| 24 | POWER STEERING SCREW | Cast iron, nodular graphite, EN GJS 800 2 | 2780 | 0.02 | 2 | 0 | 1.5 | 0.3 | 0.1 | 0.2 | 2.1 | 1.0 | 1.6 | 0.7 | 0.0 | 0.0 | 0.0 | 3.3 | >0.01-0.03 | A1 | 1 | 1 | 1 | 3 | 100 | 8042.48 | 0.00105 | 1 | 3 | 8.44 | 308.44 |
| 25 | BS EN 24014 M10 x 30 x 26-B | RS COMPONENTS: 122 4405 | - | - | 4 | 0 | 1.5 | 0.3 | 0.1 | 0.2 | 2.1 | 1.0 | 1.6 | 0.0 | 0.0 | 0.0 | 0.6 | 3.2 | - | - | - | - | - | - | - | - | - | - | - | - | - |
| 26 | BS EN 24014 - M16 x 100 x 38-N | RS COMPONENTS: 122 4498 | - | - | 1 | 0 | 1.5 | 0.3 | 0.1 | 0.2 | 2.1 | 1.0 | 1.6 | 0.0 | 0.0 | 0.0 | 0.6 | 3.2 | - | - | - | - | - | - | - | - | - | - | - | - | - |
| 27 | BS EN 24034 - M16 - N | RS COMPONENTS: 122 4425 | - | - | 1 | 0 | 1.5 | 0.3 | 0.1 | 0.2 | 2.1 | 1.0 | 1.6 | 0.0 | 0.0 | 0.0 | 0.6 | 3.2 | - | - | - | - | - | - | - | - | - | - | - | - | - |
| 28 | TIRE | Aero trainer (AD4D4) | - | - | 1 | 1 | 3 | 0.6 | 0 | 0 | 3.6 | 3.3 | 0.0 | 0.0 | 0.0 | 0.0 | 0.6 | 3.9 | - | - | - | - | - | - | - | - | - | - | - | - | - |
| 29 | WHEEL RIM | Wheel Wright (TI37-1548) | - | - | 1 | 1 | 3 | 0 | 0 | 0 | 3 | 3.3 | 0.0 | 0.0 | 0.0 | 0.0 | 0.6 | 3.9 | - | - | - | - | - | - | - | - | - | - | - | - | - |
| 30 | WHEEL BRACKET | Aluminum, 2024, T3 | 2750 | 15.43 | 1 | 0 | 1.5 | 0 | 0.1 | 0 | 1.6 | 1.0 | 1.6 | 0.0 | 0.0 | 0.0 | 0.0 | 2.6 | >1.0-3.0 | B4 | 2.3 | 2 | 1 | 2 | 151 | 5609389.19 | 0.00243 | 1.2 | 9.2 | 16356.98 | 17746.18 |
| 31 | BRAKE DISC | Tolomatic (0803-1214) | - | - | 1 | 1 | 1.5 | 0 | 0 | 0 | 1.5 | 6.0 | 1.6 | 0.0 | 1.5 | 0.7 | 0.6 | 10.4 | - | - | - | - | - | - | - | - | - | - | - | - | - |
| 32 | BRAKE CALIPER | Tolomatic (H220SAFCIG) | - | - | 1 | 1 | 1.5 | 0 | 0.1 | 0.2 | 1.8 | 6.0 | 1.6 | 0.7 | 1.5 | 0.7 | 0.6 | 11.1 | - | - | - | - | - | - | - | - | - | - | - | - | - |
| 33 | PAD NORMAL | Tolomatic (0803-1214) | - | - | 2 | 1 | 1.5 | 0 | 0.1 | 0.2 | 1.8 | 6.0 | 1.6 | 0.0 | 1.5 | 0.0 | 0.0 | 9.1 | - | - | - | - | - | - | - | - | - | - | - | - | - |
| 34 | WHEEL AXLE | AISI Type 316L Stainless steel | - | - | 1 | 1 | 1.5 | 0.2 | 0 | 0.1 | 1.8 | 1.0 | 0.0 | 0.7 | 1.5 | 0.0 | 0.0 | 3.2 | >3.0-5.0 | A1 | 1 | 1 | 1 | 2 | 18 | 962112.75 | 0.00105 | 1.1 | 2 | 1111.24 | 1147.24 |
| 35 | BALL BEARING | RS COMPONENTS: 618-9957 | - | - | 2 | 0 | 1.5 | 0.2 | 0.1 | 0.1 | 1.9 | 2.0 | 0.0 | 1.2 | 1.5 | 0.0 | 0.0 | 4.7 | - | - | - | - | - | - | - | - | - | - | - | - | - |
| 36 | BS EN 24014 - M6 x 30 x 18-B | RS COMPONENTS: 520-144 | - | - | 5 | 0 | 1.5 | 0.3 | 0.1 | 0.2 | 2.1 | 1.0 | 0.1 | 0.0 | 0.0 | 0.0 | 0.6 | 1.7 | - | - | - | - | - | - | - | - | - | - | - | - | - |
| 37 | BS EN 24014 - M6 x 45 x 18-B | RS COMPONENTS: 520-144 | - | - | 2 | 0 | 1.5 | 0.3 | 0.1 | 0.2 | 2.1 | 1.0 | 0.1 | 0.0 | 0.0 | 0.0 | 0.6 | 1.7 | - | - | - | - | - | - | - | - | - | - | - | - | - |
| 38 | BS EN ISO - 4161 - M20 - N | RS COMPONENTS: 508-1307 | - | - | 2 | 0 | 1.5 | 0.3 | 0.1 | 0.2 | 2.1 | 1.0 | 0.1 | 0.0 | 0.0 | 0.0 | 0.6 | 1.7 | - | - | - | - | - | - | - | - | - | - | - | - | - |
| 39 | BS EN 24014 - M16 x 80 x 38-B | RS COMPONENTS: 508-1177 | - | - | 1 | 0 | 1.5 | 0.3 | 0.1 | 0.2 | 2.1 | 1.0 | 0.1 | 0.0 | 0.0 | 0.0 | 0.6 | 1.7 | - | - | - | - | - | - | - | - | - | - | - | - | - |
| | | Number of Components | | | 60 | Feeding Ratio | | | | | 4.62 | Fitting Ratio | | | | | | 11.3 | | | | | | | Highest Manufacturing Index | | | | | | 161368.4 |
| | | Design Efficiency (%) | | | 20.8% | | | | | | | | | | | | | | | | | | | | Sum of Manufacturing Index | | | | | | 249293.4 |

## APPENDIX B – Lucas Analysis Detailed Calculation Table

| ITEM NO. | PART NAME | MATERIAL | DENSITY | MASS | QTY | ESL | HANDLING INDEX | | | | | FITTING INDEX | | | | | | | TOLERANCE | BAND | Rc | | | | Pc | Mc | | | MANUFACTURING COST INDEX | | |
|---|---|---|---|---|---|---|---|---|---|---|---|---|---|---|---|---|---|---|---|---|---|---|---|---|---|---|---|---|---|---|---|
| | | | kg/m3 | kg | | E | A | B | C | D | Total | A | B | C | D | E | F | Total | SFCE FINISH | | Cc | Cmp | Cs | Ct or Cf | | Volume (mm3) | Cmt | Wc | Rc | Mc | Mi |
| 1 | BS EN 24034 - M20 - N | Stainless steel, austenitic, AISI 302, HT grade B | - | - | 4 | 0 | 1.5 | 0.4 | 0.1 | 0.0 | 2.0 | 1.0 | 0.1 | 0.7 | 0.0 | 0.0 | 0.6 | 2.4 | - | - | - | - | - | - | - | - | - | - | - | - | - |
| 2 | BALL BEARING 2 | RS COMPONENTS: 618-9963 | - | - | 2 | 0 | 1.0 | 0.2 | 0.0 | 0.0 | 1.2 | 1.0 | 0.1 | 1.2 | 1.5 | 0.0 | 0.0 | 3.8 | - | - | - | - | - | - | - | - | - | - | - | - | - |
| 3 | BEARING HOLDER | Cast iron, austempered ductile, ADI 1050 | 7030 | 1.28 | 1 | 0 | 1.0 | 0.0 | 0.1 | 0.0 | 1.1 | 1.0 | 1.2 | 0.0 | 1.5 | 0.0 | 0.0 | 3.7 | >0.08-0.15 | A1 | 1 | 1 | 1 | 2 | 100 | 182692.54 | 0.00105 | 1 | 2 | 191.83 | 391.83 |
| 4 | MAIN ACTUATOR | Thomson (HD12B160-0400CNO1EEM) | - | - | 1 | 1 | 1.0 | 0.0 | 0.1 | 0.2 | 1.3 | 3.3 | 0.0 | 0.0 | 0.0 | 0.0 | 0.0 | 3.3 | - | - | - | - | - | - | - | - | - | - | - | - | - |
| 5 | UPPER L.GEAR LEVER | Aluminum, 6005, T1 | 2680 | 1.90 | 2 | 1 | 1.0 | 0.0 | 0.1 | 0.2 | 1.3 | 3.3 | 0.0 | 0.7 | 0.0 | 0.0 | 0.0 | 4 | >1.0-3.0 | B3 | 2.2 | 1 | 1 | 2.3 | 151 | 709544.36 | 0.00243 | 1.1 | 5.06 | 1896.61 | 2660.67 |
| 6 | CHASSIS (RHS) | ALUMINUM 2024-T3 | 2780 | 44.84 | 1 | 1 | 1.5 | 0.0 | 0.1 | 0.2 | 1.8 | 1.0 | 0.0 | 1.2 | 0.0 | 0.0 | 0.0 | 2.2 | >5.0-10.0 | B4 | 2.3 | 1 | 1 | 1 | 151 | 16128939.41 | 0.00243 | 1.2 | 2.3 | 47031.99 | 47379.29 |
| 7 | UP/DOWN-LOCK ACTUATOR | Thomson (AA22- 05A65M0M0N) | - | - | 1 | 1 | 1.0 | 0.0 | 0.1 | 0.0 | 1.1 | 3.3 | 0.0 | 0.0 | 0.0 | 0.7 | 0.0 | 4 | - | - | - | - | - | - | - | - | - | - | - | - | - |
| 8 | BS EN 24034 - M16 - N | RS COMPONENTS: 276 768 | - | - | 2 | 0 | 1.5 | 0.4 | 0.1 | 0.0 | 2.0 | 1.0 | 0.1 | 0.0 | 1.5 | 0.0 | 0.6 | 3.2 | - | - | - | - | - | - | - | - | - | - | - | - | - |
| 9 | BS EN 24034 - M10 - B | RS COMPONENTS: 917 3163 | - | - | 4 | 0 | 1.5 | 0.4 | 0.1 | 0.0 | 2.0 | 1.0 | 0.1 | 0.0 | 1.5 | 0.0 | 0.6 | 3.2 | - | - | - | - | - | - | - | - | - | - | - | - | - |
| 10 | LOCKING PISTON HOLDER | Cast iron, austempered ductile, ADI 1050 | 7030 | 1.80 | 1 | 1 | 1.0 | 0.2 | 0.1 | 0.2 | 1.5 | 1.0 | 0.0 | 0.0 | 1.5 | 0.0 | 0.0 | 2.5 | >0.03-0.05 | A2 | 1.2 | 1 | 1.1 | 2.4 | 18 | 256717.74 | 0.00105 | 1.1 | 3.168 | 296.51 | 353.53 |
| 11 | BS EN 24034 - M50 - B | RS COMPONENTS: 917 3019 | - | - | 1 | 0 | 1.5 | 0.0 | 0.1 | 0.0 | 1.6 | 1.0 | 0.1 | 0.7 | 0.0 | 0.0 | 0.6 | 2.4 | - | - | - | - | - | - | - | - | - | - | - | - | - |
| 12 | LOWER L.GEAR LEVER | ALUMINUM 2024-T3 | 2780 | 3.40 | 1 | 1 | 1.0 | 0.0 | 0.1 | 0.2 | 1.3 | 1.0 | 0.1 | 0.7 | 0.0 | 0.0 | 0.0 | 1.8 | >0.08-0.15 | B4 | 2.3 | 1 | 1 | 2.4 | 151 | 1222392.31 | 0.00243 | 1.2 | 5.52 | 3564.50 | 4398.02 |
| 13 | BS EN 24034 - M20 - B | RS COMPONENTS: 508 1307 | - | - | 2 | 0 | 1.5 | 0.4 | 0.1 | 0.0 | 2.0 | 1.0 | 0.1 | 0.0 | 0.0 | 0.0 | 0.6 | 1.7 | - | - | - | - | - | - | - | - | - | - | - | - | - |
| 14 | BS EN 24034 - M16 - B | RS COMPONENTS: 508 1256 | - | - | 2 | 0 | 1.5 | 0.4 | 0.1 | 0.0 | 2.0 | 1.0 | 0.1 | 0.0 | 0.0 | 0.0 | 0.6 | 1.7 | - | - | - | - | - | - | - | - | - | - | - | - | - |
| 15 | SHOCK STRUT | Aluminum ALLOY 1350 | 2700 | 32.61 | 1 | 1 | 1.0 | 0.0 | 0.1 | 0.2 | 1.3 | 3.3 | 0.0 | 0.0 | 0.0 | 0.0 | 0.0 | 3.3 | >1.0-3.0 | A3 | 2.3 | 1 | 1 | 1.9 | 151 | 12076883.21 | 0.00243 | 1.2 | 4.37 | 35216.19 | 35876.06 |
| 16 | STEERING ROTATOR | ALUMINUM 2024-T3 | 2780 | 0.80 | 1 | 1 | 1.0 | 0.0 | 0.1 | 0.2 | 1.3 | 3.3 | 0.1 | 0.7 | 0.0 | 0.0 | 0.0 | 4.1 | >1.0-3.0 | A2 | 2.1 | 1 | 1 | 1.9 | 151 | 287045.88 | 0.00243 | 1.1 | 3.99 | 767.27 | 1369.76 |
| 17 | POWER STEERING SCREW | AISI Type 316L Stainless steel | 8027 | 0.06 | 4 | 0 | 1.5 | 0.4 | 0.1 | 0.0 | 2.0 | 1.0 | 0.0 | 0.0 | 1.5 | 0.0 | 0.0 | 2.5 | >0.08-0.15 | A1 | 1 | 4 | 1 | 1 | 10 | 8042.48 | 0.00341 | 1.6 | 4 | 43.88 | 83.88 |
| 18 | POWER STEERING ACTUATOR | Thomson (AA42- 21B65M0M0B) | | | 2 | 1 | 1.0 | 0.0 | 0.1 | 0.2 | 1.3 | 1.0 | 0.1 | 0.0 | 0.0 | 0.7 | 0.0 | 1.8 | - | - | - | - | - | - | - | - | - | - | - | - | - |
| 19 | STEERING CONNECTOR | AISI Type 316L Stainless steel | 8027 | 1.37 | 2 | 1 | 1.0 | 0.0 | 0.1 | 0.2 | 1.3 | 1.0 | 0.0 | 0.7 | 0.0 | 0.7 | 0.0 | 2.4 | >1.0-3.0 | C2 | 1.4 | 4 | 1 | 1 | 10 | 171239.19 | 0.00341 | 2.4 | 5.6 | 1401.42 | 1457.42 |
| 20 | TORSION LINK CONNECTOR | AISI Type 316L Stainless steel | 8027 | 1.71 | 2 | 1 | 1.0 | 0.0 | 0.1 | 0.2 | 1.3 | 1.0 | 0.1 | 0.0 | 0.0 | 0.0 | 0.0 | 1.1 | >3.0-5.0 | A2 | 1.2 | 4 | 1 | 1 | 10 | 212864.3 | 0.00341 | 2 | 4.8 | 1451.73 | 1499.73 |
| 21 | UPPER TORQUE LINK | Carbon-fiber-reinforced polymer | 1100 | 0.11 | 1 | 1 | 1 | 0 | 0 | 0 | 1.1 | 3.3 | 0.1 | 0.7 | 0.0 | 0.7 | 0.0 | 4.8 | >3.0-5.0 | B3 | 1.8 | 1.5 | 1 | 1 | 100 | 101034.04 | 0.00035 | 1.1 | 2.7 | 38.90 | 308.90 |
| 22 | WHEEL BRACKET | Aluminum ALLOY 1350 | 2700 | 25.36 | 1 | 0 | 1.5 | 0.0 | 0.1 | 0.2 | 1.8 | 3.3 | 0.1 | 0.7 | 0.0 | 0.0 | 0.0 | 4.1 | >0.03-0.05 | B4 | 2.3 | 1 | 1 | 2.3 | 151 | 9391419.22 | 0.00243 | 1.2 | 5.29 | 27385.38 | 28184.17 |
| 23 | LOWER TORQUE LINK | Aluminum ALLOY 1350 | 1100 | 0.13 | 1 | 1 | 1 | 0 | 0 | 0 | 1.1 | 3.3 | 0.1 | 0.7 | 0.0 | 0.7 | 0.6 | 5.4 | >3.0-5.0 | B3 | 1.8 | 1.5 | 1 | 1 | 100 | 116079.66 | 0.00035 | 1.1 | 2.7 | 44.69 | 314.69 |
| 24 | BS EN 24034 - M10 - N | RS COMPONENTS: 122 4405 | - | - | 4 | 0 | 1.5 | 0.4 | 0.1 | 0.0 | 2.0 | 1.0 | 0.1 | 0.0 | 0.0 | 0.0 | 0.6 | 1.7 | - | - | - | - | - | - | - | - | - | - | - | - | - |
| 25 | TIRE | Aero trainer (AD4D4) | - | - | 1 | 1 | 1.5 | 0.6 | 0.0 | 0.0 | 2.1 | 3.3 | 0.1 | 0.0 | 0.0 | 0.0 | 0.6 | 4 | - | - | - | - | - | - | - | - | - | - | - | - | - |
| 26 | WHEEL RIM | Wheel Wright (TI37-1548) | | | 1 | 1 | 1.5 | 0.0 | 0.0 | 0.0 | 1.5 | 1.0 | 0.1 | 0.0 | 0.0 | 0.0 | 0.0 | 1.1 | - | - | - | - | - | - | - | - | - | - | - | - | - |
| 27 | BRAKE CALIPER | Tolomatic (H220SAFCIG) | - | - | 1 | 1 | 1.0 | 0.0 | 0.1 | 0.2 | 1.3 | 6.0 | 0.1 | 0.0 | 0.0 | 0.7 | 0.0 | 6.8 | - | - | - | - | - | - | - | - | - | - | - | - | - |
| 28 | BALL BEARING 1 | RS COMPONENTS: 618-9957 | - | - | 2 | 1 | 1.0 | 0.2 | 0.1 | 0.0 | 1.3 | 1.0 | 0.1 | 0.0 | 1.5 | 0.0 | 0.0 | 2.6 | - | - | - | - | - | - | - | - | - | - | - | - | - |
| 29 | BRAKE DISC | Tolomatic (0803-1214) | - | - | 1 | 1 | 1.5 | 0.0 | 0.0 | 0.0 | 1.5 | 1.0 | 0.1 | 0.7 | 0.0 | 0.0 | 0.0 | 1.8 | - | - | - | - | - | - | - | - | - | - | - | - | - |
| 30 | STRUCT CONNECTOR | Cast iron, austempered ductile, ADI 1050 | 7030 | 6.76 | 1 | 1 | 1.0 | 0.0 | 0.0 | 0.0 | 1.0 | 3.3 | 0.1 | 0.0 | 0.0 | 0.0 | 0.0 | 3.4 | >3.0-5.0 | A1 | 1 | 1 | 1 | 2 | 18 | 962112.75 | 0.00105 | 1.1 | 2 | 1111.24 | 1147.24 |
| 31 | BS EN 24034 - M50 - N | RS COMPONENTS: 917 3020 | - | - | 1 | 0 | 1.5 | 0.4 | 0.1 | 0.0 | 2.0 | 1.0 | 0.1 | 0.0 | 0.0 | 0.0 | 0.6 | 1.7 | - | - | - | - | - | - | - | - | - | - | - | - | - |
| 32 | CHASSIS (LHS) | Aluminum, 6005, T1 | 2680 | 43.22 | 1 | 1 | 1.5 | 0.0 | 0.1 | 0.2 | 1.8 | 1.0 | 0.0 | 0.7 | 0.0 | 0.0 | 0.0 | 1.7 | >5.0-10.0 | B4 | 2.3 | 1 | 1 | 1 | 151 | 16128168.11 | 0.00243 | 1.2 | 2.3 | 47029.74 | 47377.04 |
| | | **Number of Components** | | | 53 | **Feeding Ratio** | | | | | 3.48 | **Fitting Ratio** | | | | | | 5.84 | | | | | | | **Highest Manufacturing Index** | | | | | | 47379.3 |
| | | **Design Efficiency (%)** | | | 47.2% | | | | | | | | | | | | | | | | | | | | **Sum of Manufacturing Index** | | | | | | 172802.2 |

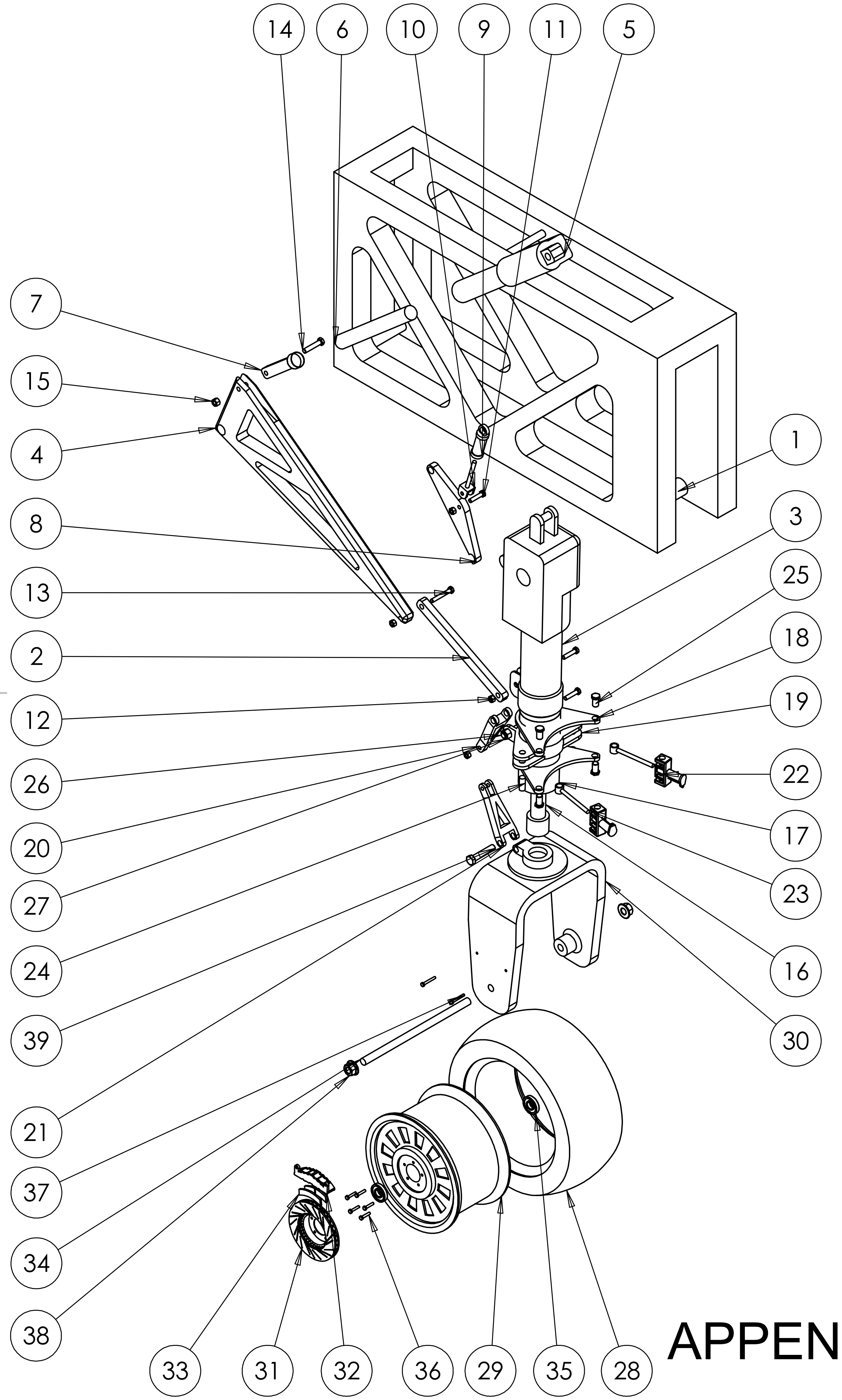


# APPENDIX C

| ITEM NO. | PART NUMBER | MATERIAL | QTY. |
|---|---|---|---|
| 1 | LANDING GEAR CHASSIS | ALUMINUM, 2024, T3 | 1 |
| 2 | LOWER L.GEAR LEVER | ALUMINUM, A201.0, CAST, T7 | 1 |
| 3 | SHOCK STRUT | ALUMINUM, 2024, T3 | 1 |
| 4 | UPPER L.GEAR LEVER | ALUMINUM, 2024, T3 | 1 |
| 5 | MAIN ACTUATOR CYLINDER | ALUMINUM, 6463, T4 | 1 |
| 6 | MAIN ACTUATOR PISTON | ALUMINUM, 6463, T4 | 1 |
| 7 | MAIN ACTUATOR GRIPPER | ALUMINUM, 6463, T4 | 1 |
| 8 | UP/DOWN-LOCK HOOK | ALUMINUM, 2024, T3 | 1 |
| 9 | UP/DOWN-LOCK CYLINDER | ALUMINUM, 2024, T3 | 1 |
| 10 | UP/DPWN-LOCK PISTON | ALUMINUM, 2024, T3 | 1 |
| 11 | BS EN 24014 - M10 X 45 X 26-B | RS COMPONENTS: 418-8104 | 3 |
| 12 | BS EN 24034 - M10 - N | RS COMPONENTS: 122-4405 | 4 |
| 13 | BS EN 24014 - M10 X 70 X 26-B | RS COMPONENTS: 418-8105 | 1 |
| 14 | BS EN 24014 - M12 X 60 X 30-B | RS COMPONENTS: 508-0994 | 1 |
| 15 | BS EN 24034 - M12 - N | RS COMPONENTS: 122-4405 | 1 |
| 16 | SHOCK STRUT PISTON | ALUMINUM, 2024, T3 | 1 |
| 17 | SHOCK STRUT CYLINDER | ALUMINUM, 2024, T3 | 1 |
| 18 | STEERING CONNECTOR | ALUMINUM, 2024, T3 | 2 |
| 19 | STEERING ROTATOR | ALUMINUM, 2024, T3 | 2 |
| 20 | UPPER TORQUE LINK | CARBON-FIBER-REINFORCED POLYMER | 1 |
| 21 | LOWER TORQUE LINK | CARBON-FIBER-REINFORCED POLYMER | 1 |
| 22 | POWER STEERING CYLINDER | ALUMINUM, 2024, T3 | 2 |
| 23 | POWER STEERING PISTON | ALUMINUM, 2024, T3 | 2 |
| 24 | POWER STEERING SCREW | CAST IRON, NODULAR GRAPHITE, EN GJS 800 2 | 2 |
| 25 | BS EN 24014 M10 x 30 x 26-B | RS COMPONENTS: 122 4405 | 4 |
| 26 | BS EN 24014 - M16 X 100 X 38-N | RS COMPONENTS: 122 4498 | 1 |
| 27 | BS EN 24034 - M16 - N | RS COMPONENTS: 122 4425 | 1 |
| 28 | TYRE | AERO TRAINER (AD4D4) | 1 |
| 29 | WHEEL RIM | WHEEL WRIGHT (TI37-1548) | 1 |
| 30 | WHEEL BRACKET | ALUMINUM, 2024, T3 | 1 |
| 31 | BRAKE DISC | TOLOMATIC (0803-1214) | 1 |
| 32 | BRAKE CALIPER | TOLOMATIC (H220SAFCIG) | 1 |
| 33 | PADNORMAL | TOLOMATIC (0803-1214) | 2 |
| 34 | WHEEL AXLE | AISI TYPE 316L STAINLESS STEEL | 1 |
| 35 | BALL BEARING | RS COMPONENTS: 618-9957 | 2 |
| 36 | BS EN 24014 - M6 X 30 X 18-B | RS COMPONENTS: 520-144 | 5 |
| 37 | BS EN 24014 - M6 X 45 X 18-B | RS COMPONENTS: 520-144 | 2 |
| 38 | BS EN ISO - 4161 - M20 - N | RS COMPONENTS: 508-1307 | 2 |
| 39 | BS EN 24014 - M16 X 80 X 38-B | RS COMPONENTS: 508-1177 | 1 |

# APPENDIX D

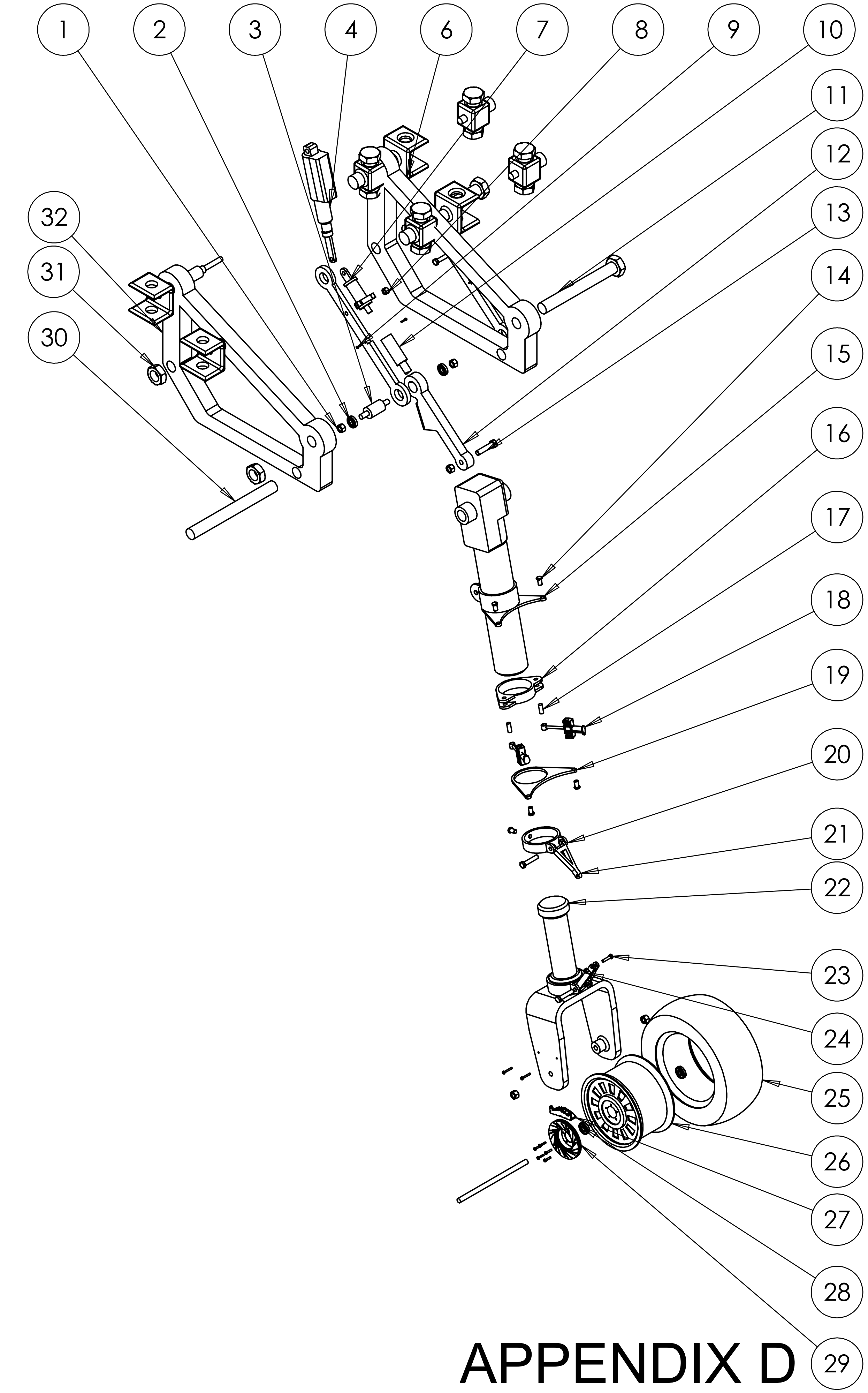

| ITEM NO. | PART NAME | MATERIAL | QTY. |
|---|---|---|---|
| 1 | BS EN 24034 - M20 - N | STAINLESS STEEL, AUSTENITIC, AISI 302, HT GRADE B | 4 |
| 2 | BALL BEARING 2 | RS COMPONENTS: 618-9963 | 2 |
| 3 | BEARING HOLDER | CAST IRON, AUSTEMPERED DUCTILE, ADI 1050 | 1 |
| 4 | MAIN ACTUATOR | THOMSON (HD12B160-0400CNO1EEM) | 1 |
| 5 | UPPER L.GEAR LEVER | ALUMINUM, 6005, T1 | 2 |
| 6 | CHASSIS (RHS) | ALUMINUM 2024-T3 | 1 |
| 7 | UP/DOWN-LOCK ACTUATOR | THOMSON (AA22- 05A65M0M0N) | 1 |
| 8 | BS EN 24034 - M16 - N | RS COMPONENTS: 276 768 | 2 |
| 9 | BS EN 24034 - M10 - B | RS COMPONENTS: 917 3163 | 4 |
| 10 | IOCKING PISTON HOLDER | CAST IRON, AUSTEMPERED DUCTILE, ADI 1050 | 1 |
| 11 | BS EN 24034 - M50 - B | RS COMPONENTS: 917 3019 | 1 |
| 12 | LOWER L.GEAR LEVER | ALUMINUM 2024-T3 | 1 |
| 13 | BS EN 24034 - M20 - B | RS COMPONENTS: 508 1307 | 2 |
| 14 | BS EN 24034 - M16 - B | RS COMPONENTS: 508 1256 | 2 |
| 15 | SHOCK STRUT | ALUMINUM ALLOY 1350 | 1 |
| 16 | STEERING ROTATOR | ALUMINUM 2024-T3 | 1 |
| 17 | POWER STEERING SCREW | AISI TYPE 316L STAINLESS STEEL | 4 |
| 18 | POWER STEERING ACTUATOR | THOMSON (AA42- 21B65M0M0B) | 2 |
| 19 | STEERING CONNECTOR | AISI TYPE 316L STAINLESS STEEL | 2 |
| 20 | TORSION LINK CONNECTOR | AISI TYPE 316L STAINLESS STEEL | 2 |
| 21 | UPPER TORQUE LINK | CARBON-FIBER-REINFORCED POLYMER | 1 |
| 22 | WHEEL BRACKET | ALUMINUM ALLOY 1350 | 1 |
| 23 | LOWER TORQUE LINK | ALUMINUM ALLOY 1350 | 1 |
| 24 | BS EN 24034 - M10 - N | RS COMPONENTS: 122 4405 | 4 |
| 25 | TIRE | AERO TRAINER (AD4D4) | 1 |
| 26 | WHEEL RIM | WHEEL WRIGHT (TI37-1548) | 1 |
| 27 | BRAKE CALIPER | TOLOMATIC (H220SAFCIG) | 1 |
| 28 | BALL BEARING 1 | RS COMPONENTS: 618-9957 | 2 |
| 29 | BRAKE DISC | TOLOMATIC (0803-1214) | 1 |
| 30 | STRUCT CONNECTOR | CAST IRON, AUSTEMPERED DUCTILE, ADI 1050 | 1 |
| 31 | BS EN 24034 - M50 - N | RS COMPONENTS: 917 3020 | 1 |
| 32 | CHASSIS (LHS) | ALUMINUM, 6005, T1 | 1 |